THE BIOLOGICAL AND DEMOGRAPHIC FACTORS DETERMINING POPULATION CONNECTIVITY IN SEA SCALLOPS (*PLACOPECTEN MAGELLANICUS*) ON GEORGES BANK

by

Chad S. Gilbert

Submitted in partial fulfillment of the requirements
for the degree of Master of Science

at

Dalhousie University
Halifax, Nova Scotia
March 2011

DALHOUSIE UNIVERSITY

DEPARTMENT OF ENGINEERING MATHEMATICS AND INTERNETWORKING

The undersigned hereby certify that they have read and recommend to the Faculty of Graduate Studies for acceptance a thesis entitled "THE BIOLOGICAL AND DEMOGRAPHIC FACTORS DETERMINING POPULATION CONNECTIVITY IN SEA SCALLOPS (*PLACOPECTEN MAGELLANICUS*) ON GEORGES BANK" by Chad S. Gilbert in partial fulfillment of the requirements for the degree of Master of Science.

Dated: March 25, 2011

Supervisor: _____

Readers: _____

_____

DALHOUSIE UNIVERSITY

DATE: March 25, 2011

AUTHOR: Chad S. Gilbert

TITLE: THE BIOLOGICAL AND DEMOGRAPHIC FACTORS DETERMINING POPULATION CONNECTIVITY IN SEA SCALLOPS (*PLACOPECTEN MAGELLANICUS*) ON GEORGES BANK

DEPARTMENT OR SCHOOL: Department of Engineering Mathematics and Internetworking

DEGREE: M.Sc. CONVOCATION: May YEAR: 2011

_____

Signature of Author

TABLE OF CONTENTS

LIST OF TABLES

LIST OF FIGURES

ABSTRACT

The Georges Bank (GB) scallop (*Placopecten magellanicus*) population is an economically valuable fishery in Canada and the US. The roles of biological factors such as larval swimming behaviour, development rates and spawning season and of demographic factors such as adult distribution and larval mortality in determining population connectivity in scallops on GB are currently unknown. In this thesis, a new particle-tracking model is developed and used to simulate larval dispersal in realistic 3D currents. It highlights the influences of biological and demographic factors, and quantifies their effects on larval dispersal and population connectivity. Larval depth-distribution and adult distribution are found to have significant impacts, and further, it is suggested that the previously overlooked spring spawning event may contribute significantly to population connectivity. These results are used to help prioritize future field, lab and modelling work that is requisite to understanding the connectivity in this metapopulation.

LIST OF ABBREVIATIONS AND SYMBOLS USED

Symbol	Units	Definition
(u, v, w)	ms^{-1}	The Lagrangian residual velocity
T	°C	Time-averaged Lagrangian Temperature
ρ	kg m^{-3}	Time-averaged Lagrangian water density
k	m^2s^{-1}	Time-averaged Lagrangian mixing coefficient
T_0	°C	Reference temperature
Q_{10}	no unit	Temperature coefficient
PLD	days	Planktonic Larval Duration
m	d^{-1}	Mortality rate
f_i	larvae scallop^{-1}	Specific fecundity of size-class i.
$c_i(x, y)$	scallops km^{-2}	Density of female scallops in size-class i at position (x, y).
$l(x, y)$	larvae km^{-2}	The spawning field, representing the density of larvae spawned at positions (x, y).
$\phi_{(i,j)}$	no units	The connection fraction linking subpopulation j to subpopulation i.
$\ell_{(i,j)}$	larvae	The migration rate of larvae from subpopulation j to subpopulation i.

GLOSSARY

connection fraction The fraction, $\phi_{(i,j)}$, of particles spawned in subpopulation j, which settle in subpopulation i. E.g. "The connection fraction from NEP to GSC was 10%". 28, 75

dispersal The spread of larvae from a spawning source to a set of of settlement sites. See *Pineda et al.* (2007) for details. 2

large scallops Scallops having shell height between 120-170 mm. 22

larval connectivity The degree to which populations are connected via larval exchange, neglecting settlement and post-settlement processes. See appendix B for details. 29

larval production field The density of larvae spawned, described as a function $l(x, y)$. The domain is the set of points (x, y) that are located in a subpopulation. 22

macroscale Spatial scales on the order of tens to hundres of kilometers. 7

medium scallops Scallops having shell height between 95-120 mm. 22

mesoscale Spatial scales on the order of kilometers to tens of kilometers. 7

metapopulation A suitable definition for "metapopulation" is the subject of debate in the literature (*Grimm et al.*, 2003; *Kritzer and Sale*, 2004). One definition is offered by *Kritzer and Sale* (2004): "*the critical feature of metapopulations is the coupling of spatial scales, whereby local populations [subpopulations] experience partially independent dynamics but receive some identifiable demographic influence from other populations.*" It is unclear whether the scallop population on GB satisfies this definition, in part because not enough is yet known about the dispersal of its larvae. It may turn out that the scallops on GB are better described simply as one single "spatially structured" population (*Grimm et al.*, 2003). The metapopulation label is used in this thesis for referring to the set of interacting subpopulations on GB. 2

migration rate The number, $\ell_{(i,j)}$, of larvae spawned in a subpopulation j, which settled in a subpopulation i. E.g. "The migration rate from NEP to GSC was 1 billion larvae". 29, 55

population connectivity The degree to which populations are connected through migration. See appendix B for details. 2, 72

post-closures era The years following the implementation of fishery closed areas in the US Georges Bank. In this thesis, these are specifically the years 1996-2004. 5

pre-closures era The years from 1984 to 1994, during which fishery landings in the US Georges Bank were relatively low before the implementation of fishery closed areas. 5

recruitment In general, recruitment refers to the addition of new members to a population. For *P. magellanicus*, this is usually defined as the survival of a juvenile scallop to 2-3 years of age (80 mm), at which time it becomes available to the fishery (*Hart*, 2006). 5, 72

settlement distribution The distribution of particles or simulated larvae in space at the end of their simulated larval duration. 27

settlement position The position of larva at the end of its simulated PLD. If significant transport occurs during or after the pediveliger phase, then this may not be the true final position of the scallop, and can be thought of as the position at which settlement behaviour is initialized. 27

small scallops Scallops having shell height between 50-95 mm. 22

subpopulation A geographically delimited subset of individuals from within some larger population. 2

transport The movement of a larva from one geographical position to another. See *Pineda et al.* (2007) for details. 2

transport connectivity The degree to which populations are connected transport, neglecting all demographic processes such as spawning and mortality. See appendix B for details. 28

ACKNOWLEDGEMENTS

First and foremost, I thank my thesis supervisor, Dr. Wendy C. Gentleman for encouraging me to dive head-first into studying oceanography and for ensuring I don't drown in the process. In addition to her deep technical knowledge, she has shared with me her wisdom and her extremely contagious enthusiasm for science.

My supervisors and mentors, Drs. Catherine L. Johnson and Claudio DiBacco, consistently helped and challenged me to think in new ways. I am forever grateful for their investments of time, patience and expertise.

Drs. Gordon Fenton, Charles Hannah, Dan Kelley, Anna Neuheimer, Jamie Pringle and Jinyu Sheng have all contributed significant teaching and mentorship, which added greatly to my understanding of various aspects of the science and methods found this thesis.

I am also grateful for various contributions of time and knowledge from Jason Chaffey, Changshen Chen, Alex Curtis, Jennifer Fitzgerald, Dvora Hart, Erica Head, Ed Houde, Ian Jonsen, Blake MacDonald, Leslie Nasmith, Elizabeth North, Stephen Smith, Kathleen Svendsen and John Tremblay. These people have all demonstrated true scientific spirit in sharing with me their knowledge, ideas and data. Thanks also to Kelly Lynch for helping me wrestle with several unruly sentences that appeared in earlier drafts of this thesis to finally pin them down and force them to make some sense.

I thank Dr. William Phillips, Mrs. Karen Conrod and the rest of the faculty in the Engineering Mathematics Department, Dalhousie University for providing such a positive and productive work environment.

I thank everyone at the Dalhousie University Oceanography Department – the students, professors and administration – for welcoming me into their classes, their talks and their offices. And more importantly, for their friendship.

This research has been funded by a NSERC postgraduate scholarship, Fisheries and Oceans, Canada and the Department of Engineering Mathematics & Internetworking, Dalhousie University. I am grateful for the financial support of all of these institutions.

CHAPTER 1

INTRODUCTION

In the previous three decades, commercial sea scallop (*Placopecten magellanicus*) stocks on Georges Bank (GB) have provided annual landings ranging between 8,000 to 28,000 metric tons of meats for the combined Canadian and US fisheries (*Naidu and Robert*, 2006), with an estimated value on the order of $100-$300 M per year in today's dollars. Additionally, the success of fisheries downstream of GB may depend on the health of this resource (*Tian et al.*, 2009a). The large value of the fishery justifies much interest in understanding the dynamics of this population, and how it is impacted by anthropogenic, ecological, and climatic factors.

Figure 1.1: An image of the giant sea scallop *P. magellanicus*. Photograph by Dann Blackwood, USGS

Though the adults are sedentary (they live on the sea floor and do not migrate significantly), they spawn planktonic larvae that are subject to *dispersal* in ocean currents (see Appendix A for details). It follows that recruits to any local *subpopulation* are not necessarily spawned locally, and so the local population dynamics can not be understood without considering interactions between the subpopulations. Rather, the scallop population on GB is better thought of as a connected network of subpopulations that function together as one larger *metapopulation*. A quantitative characterization of this interconnectedness between subpopulations (of the *population connectivity*; see appendix B) is considered to be crucial to the success of certain types of management strategies such as marine-protected areas (*Botsford et al.*, 2001), to understanding the ecological role of scallop larvae, and to understanding the dynamics of the population (*Cowen and Sponaugle*, 2009).

There are severe practical limitations associated with characterizing population connectivity empirically because larval *transport* cannot be easily observed (*Werner et al.*, 2007). Thus, computer modelling and simulation approaches are being developed to supplement gaps in our knowledge. These models synthesize observations and theory from the literature in attempt to rationally derive implications that are held therein. However, modellers are forced to make simplifying assumptions to deal with the complexity in larval behaviour, demographics and the environment of scallops. This leaves a great deal of uncertainty in interpreting attempts at prediction and diagnosis of population connectivity in scallops on GB. Therefore, the sensitivity of models to these assumptions must be understood if their results are to be linked to reality and used sensibly in support of fishery management policies and in guiding future research.

Previous efforts to characterize scallop larval dispersal on GB have been made (*Tremblay et al.*, 1994; *Lewis*, 1999; *Tian et al.*, 2009a,b,c). *Tremblay et al.* (1994) focused on characterizing larval retention within the GB population by simulating larval drift in a hydrodynamic model. Following the implementation of fishery closed areas on GB in 1994,

Lewis (1999) performed a complementary study which examined the exchange of scallop larvae between the closed areas. *Tian et al.* (2009a,b) added some complexity to both of these studies by investigating the effects of inter-annual hydrodynamic variation on larval retention within GB and on exchange between the closed areas, and showed that larval dispersal is sensitive to to these fluctuations. The new focus on the impact of environmental variability on larval dispersal raises the complementary question: *how crucial are changes in biological and demographic factors in determining larval dispersal and connectivity among GB scallop subpopulations?* In this dissertation, six such biological/demographic factors are identified (three which might be classed as "biological" and three more as "demographic") and their impacts evaluated through model investigation.

1.1 Background and Motivation

There are three major scallop aggregations on GB, which are referred to in this thesis as distinct subpopulations (*Tremblay et al.*, 1994; *Hart and Chute*, 2004). Transport of larvae among these subpopulations is principally driven by the tidal mixing front recirculation, along-shelf currents, and wind-induced variation in surface flows (*Tremblay et al.*, 1994; *Tian et al.*, 2009a). Previous studies indicate that the scallop aggregation residing in the Great South Channel (GSC; figure 1.2) is the most retentive, receiving larvae spawned from the Northeast Peak (NEP; figure 1.2) and Southern Flank (SF; figure 1.2) stocks, as well as retaining locally spawned larvae (*Tremblay et al.*, 1994). In contrast, the models suggest local retention of larvae spawned in the NEP is unlikely, that in SF subpopulations is negligible, and they both rely primarily on input of larvae spawned in the GSC (*Tremblay et al.*, 1994; *Tian et al.*, 2009a). However, this finding conflicts with another study in which spawning on the NEP was positively related to local recruitment two years later (*Mcgarvey et al.*, 1993). Larval supply from scallops beds upstream of GB could contribute to recruitment in these aggregations, though surveys of larval abundance in Georges Basin

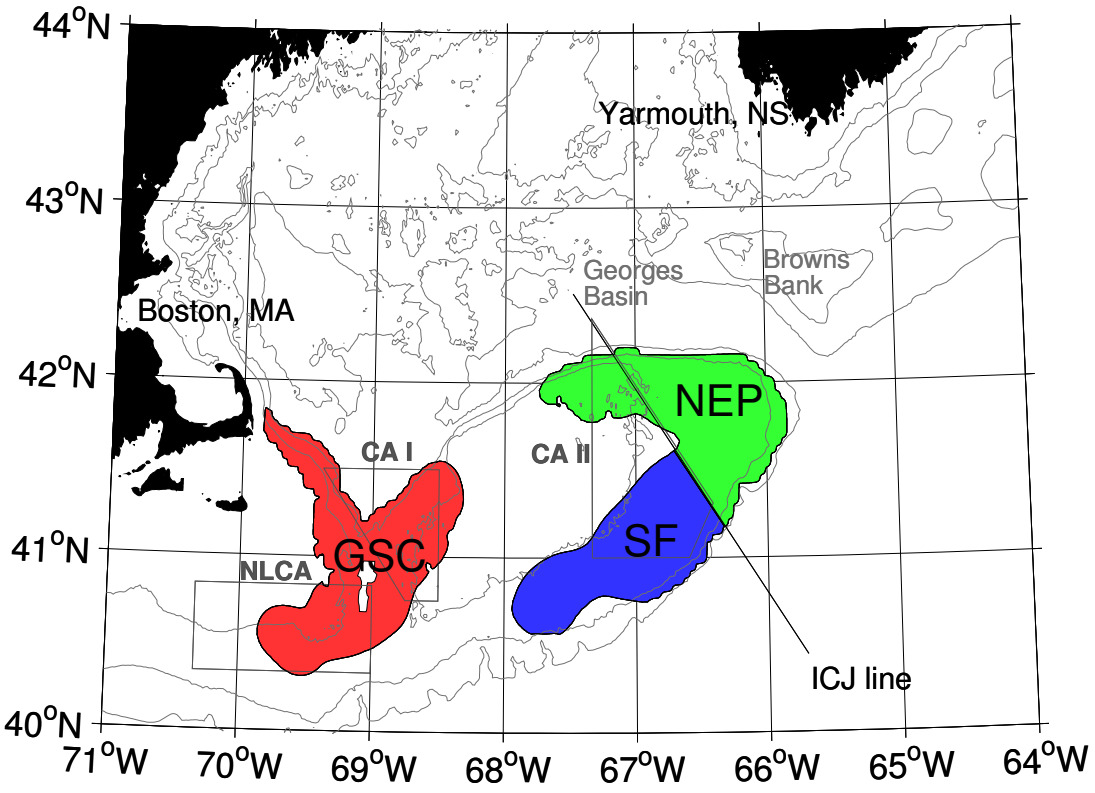

Figure 1.2: A map of Georges Bank. The three major scallop aggregations on GB are located in the Great South Channel (GSC, red), the Northeast Peak (NEP, green) and the Southern Flank (SFL, blue). Bathymetry contours are plotted at 60, 100 and 200 meters depth. To provide familiar references, the approximate locations of Boston, Massachusetts and Yarmouth, Nova Scotia are labelled on the map. Three fishery closed areas are shown – the Nantucket Lightship Closed Area (NLCA), Closed Area I (CA I) and Closed Area II (CA II). The international court of justice (ICJ) line divides the exclusive economic zones of Canada and the US (*International Court of Justice*, 1984).

in the years 1985-1987 suggest that upstream supply of scallop larvae from Browns Bank to GB is limited (*Tremblay and Sinclair*, 1992). The potential for scallop populations from the Gulf of Maine to seed GB is unknown.

Exchange patterns of *P. magellanicus* larvae on GB depend on environmental conditions – variation in the winds and stratification affect GB circulation (*Naimie et al.*, 1994, 2001; *Pringle*, 2006). Simulations of larval dispersal on GB suggested that the number of larvae retained on the bank until settlement can change in each year, with up to five times more larvae retained in a good year than in a bad year (*Tian et al.*, 2009a). High frequency variation in the currents, which are typically ignored in particle-tracking studies on GB, also

have non-negligible effects on larval dispersal (*Tian et al.*, 2009c). Moreover, variations in temperature and/or stratification may elicit different biological responses, and previous studies indicate that changes in swimming behaviour and growth rate can have significant effects on larval transport (e.g. *Tremblay et al.*, 1994; *Tian et al.*, 2009a).

Scallop biomass has historically been the highest on the NEP, which has been part of the Canadian exclusive economic zone since 1984 (*International Court of Justice*, 1984). However, the US portion of GB has experienced a significant increase in scallop biomass in both the GSC and SF since three area closures were implemented in 1994. Most ($\sim$80%) larvae spawned in CA I and the northern part of CA II are retained within GB (average over 11 years; *Tian et al.*, 2009b). No significant evidence was found for an increase in the rate of *recruitment* on GB in the *post-closures era* (1996-2004), relative to the *pre-closures era* (1984-1994) (*Hart and Rago*, 2006). The increase in biomass was therefore attributed primarily to a lower mortality rate among existing scallops. The lack of increased recruitment was attributed to density-dependent inhibition under the assumption that the increase in scallop biomass had led to an increase in the number of larvae being retained within the population (*Stokesbury et al.*, 2004; *Hart and Rago*, 2006).

1.1.1 Depth Distribution

Larval depth-distribution can influence dispersal because of vertical shear in the currents. Model sensitivity analyses that compared the effects of different hypothetical swimming behaviours (e.g. passive, fixed depth, surface-seeking) on dispersal of *P. magellanicus* larvae demonstrated significant sensitivity (*Tremblay et al.*, 1994). Retention on GB was lower for shallower larvae, higher for larvae deeper in the water-column, and the amount of larval exchange among the aggregations varied by $\sim$50% among the different simulated behaviours (*Tremblay et al.*, 1994; *Tian et al.*, 2009a). More study on the influence of depth-distribution is needed because behaviours simulated in previous studies were simplified

and may not have been sufficiently realistic (*Tremblay et al.*, 1994). For example, no simulations have been made in which larvae maintain themselves near the pycnocline, as would be consistent with field observations (*Tremblay and Sinclair*, 1990).

1.1.2 Planktonic Larval Duration

For scallops, the planktonic larval duration (PLD) corresponds to the development time from hatch to settlement, which varies with temperature (*Tremblay et al.*, 1994). The PLD of *P. magellanicus* on GB is typically assumed to be $\sim$35 d in the fall based on mean temperature (*Tremblay et al.*, 1994), but changes in this value of PLD affect simulated larval drift. A shorter PLD reduces dispersal distances, increasing the connectivity from GSC to NEP, whereas a longer PLD is associated with increased loss of larvae from GB (*Tremblay et al.*, 1994). Because temperatures on GB exhibit pronounced spatial and temporal variability (*Naimie et al.*, 1994), PLDs likely vary among individuals due to differences in their thermal histories (*Neuheimer and Taggart*, 2007; *Metaxas and Saunders*, 2009). However, the effect that individual variation in PLD has on larval dispersal has not been investigated.

1.1.3 Transport in Spring

All previous modelling of *P. magellanicus* has been limited to larvae spawned in the fall (mid-September; *Tremblay et al.*, 1994; *Tian et al.*, 2009a,c). However, scallops also spawn in spring (April-June; *DiBacco et al.*, 1995). One reason that was offered for the focus on fall-spawned larvae was that the gyre that drives recirculation on GB is weaker in spring, and would presumably lead to lower retention of larvae within the metapopulation (*Tremblay et al.*, 1994). This seems to conflict with the fact that spring spawning behaviour exhibited by scallops on GB persists. If spring spawning did not increase the expected number of progeny for the scallops, it would presumably be selected

out of the population. Circulation in the spring is generally in the same direction as that in fall, though residual currents are slower and the around-bank gyre is weaker prior to the development of stratification (*Naimie et al.*, 1994, 2001). Dispersal of larval scallops in the spring is likely dependent on depth-distributions and PLD, as these factors have been shown to be critical for other planktonic species on GB in this season (*Werner et al.*, 1993; *Miller et al.*, 1998; *Lynch et al.*, 1998; *Lough and Manning*, 2001). However, the influence of currents typical of the spring on larval transport has yet to be assessed quantitatively.

1.1.4 Spatially Heterogeneous Spawning

The spatial scale associated with the subpopulations on GB (tens to hundreds of kilometers) is typically referred to as the *macroscale* (*Orensanz et al.*, 2006). However, there is also noticeable spatial structure within these subpopulations at the *mesoscale*, which is on the order of kilometers (*Adams et al.*, 2010). Previous modelling studies (*Tremblay et al.*, 1994) have divided the GB metapopulation up into three distinct subpopulations (GSC, NEP, SF) at the macroscale and investigated the potential for larval exchange among them. However, it is already clear that smaller scale ocean currents on GB influence larval transport (*Tian et al.*, 2009c), which suggests that the location of spawning within a subpopulation can play a fundamental role in determining the fates of larvae. The fact that larval production within each subpopulation is spatially heterogeneous suggests that accurate estimation of larval connectivity may require that the spatial distribution of spawning adults be considered, as opposed to just the total number present within within each subpopulation. The relative importance of obtaining an accurate estimate of the spatial distribution of spawning within each subpopulation has yet to be evaluated.

1.1.5 Larval Production and Survivorship in Spring

Seasonal differences in production and survival to settlement size of scallop larvae may impact the relative contribution of spring spawned larvae to population connectivity on GB.

The spring spawning event is characteristically smaller than that in the fall, with fewer eggs being released by reproductive females (*DiBacco et al.*, 1995). A longer PLD in spring would also suggest lower net survivorship if larval mortality rates are assumed to be similar in both seasons. Larval mortality rates *in situ* for either season are not known. However, the environment on GB in each season is different physically (*Naimie et al.*, 1994) and ecologically (*Davis*, 1987), and the larvae may encounter different abiotic factors, as well as different types and abundances of predators and prey that could control mortality. The relative contribution of spring spawned larvae to population connectivity and its sensitivity to assumptions about inter-seasonal differences in fecundity and larval mortality have yet to be evaluated.

1.1.6 Larval Connectivity Across Fishery Eras

The increase in scallop biomass that occurred in the *post-closures* era on the US portion of GB was attributed in large part to an increase in the mean size of the scallops (*Hart and Rago*, 2006). Increases in either abundance or mean size suggest a corresponding increase in larval production, since fecundity is strongly correlated with shell height (*Langton et al.*, 1987). Though more larvae were produced during the *post-closures* era, no significant increase in recruitment was observed (*Hart and Rago*, 2006). It is already suggested that larvae spawned in the closed areas are likely retained on GB (*Tian et al.*, 2009b); however, the location of settlement within GB has a significant impact on settlement success and post-settlement survival (*Thouzeau et al.*, 1991). There are therefore two possible explanations for the lack of increased recruitment on GB: density-dependent inhibition, or no increase in the number of larvae arriving to settle. The particle-tracking model developed in this thesis provides an opportunity to run a case study: evaluating the impact that the fishery closed areas have had on larval supply within the metapopulation.

1.2 Objectives & Outline

The aim of this thesis is to provide insight into the six major questions raised in section 1.1. These can be summarized:

1. How does switching from a *passive* to a *pycnocline-seeking* swimming behaviour impact larval transport? (chapter 3)

2. Does individually-varying temperature-dependent PLD influence larval dispersal? (chapter 3)

3. How is larval dispersal in spring different from that in fall? (chapter 3)

4. Does mesoscale variation in scallop distribution affect larval dispersal? (chapter 4)

5. How does larval connectivity in spring compare to that in fall? (chapter 4)

6. How has larval connectivity been changed by the US fishery closed areas? (chapter 4)

To address these questions, a new individual-based particle-tracking model was developed, which simulates the production, transport and mortality of scallop larvae on GB. This model and the simulation strategy are described in detail in chapter 2. Chapter 3 evaluates the sensitivity of scallop larval dispersal and settlement within three subpopulations to three biological factors (larval swimming behaviour, planktonic larval duration and spawning seasonality), and questions 1-3 are addressed. These results are already published (*Gilbert et al.*, 2010), but were performed explicitly as a part of this thesis work and represent substantial original contributions to the research and writing on the part of the author. Chapter 4 evaluates the sensitivity of larval dispersal and connectivity between the three subpopulations to three demographic factors (mesoscale variation in scallop distribution, seasonally varying fecundity and larval mortality rate, and historical change in scallop abundance and distribution), allowing questions 4-6 to be adressed. Finally, chapter 5

summarizes the findings and puts them in context, identifying potential avenues for further empirical and modelling work on population connectivity in scallops on GB.

This thesis also contains four appendices. Appendix A provides some relevant background information on the life-history characteristics of *P. magellanicus* that are needed to understand the modelling assumptions made in this dissertation. Next, appendix B explains several key terms used throughout this thesis (such as transport connectivity, larval connectivity), all of which are related to the concept of population connectivity. Appendix C contains the rights release form from Elsevier, the publisher of *Gilbert et al.* (2010), giving permission to reproduce the contents of that paper here. Appendix D describes the "Lagrangian Residual Velocity", and explains how this quantity was used to efficiently simulate larval transport.

CHAPTER 2

METHODS

The six major questions of this thesis were addressed by simulating larval dispersal in an individual-based particle-tracking model. The individual-based particle-tracking model is a computer program in which interactions between scallop larvae and their physical environment are simulated. Dispersal is the result of spawning, transport, growth, mortality and settlement behaviour of larvae (*Pineda et al.*, 2007), so each of these processes was simulated in the program. A conceptual diagram of the model is given in figure 2.1. Controlled 'numerical experiments' were run by making changes to the model and analyzing their effects on simulated dispersal.

The physical environment was simulated in a hydrodynamic model in which the currents, turbulence, temperature and density of water in the Georges Bank region are represented in three spatial dimensions and in time. The relevant details of the hydrodynamic model setup and of the resulting simulated environment are given in section 2.1.

In chapter 3, individual larvae were represented in the computer program as a set of numerical values: the position, (x, y, z), and size, s. Changes in these values over time represent transport and growth of the larva. For the simulations in chapter 4, individual larvae were replaced by super-individuals, which are taken to represent a number of individuals, n. A review of the super-individual concept is given by *Scheffer* (1995).

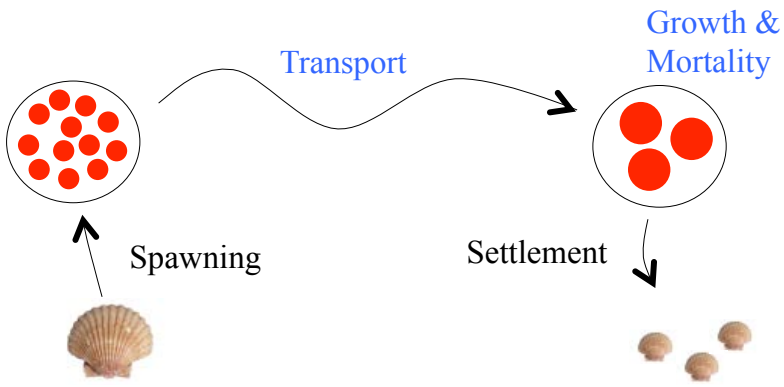

Figure 2.1: A conceptual diagram of the indiviual-based particle tracking model developed for this thesis. Super-individuals undergo growth and mortality during transport (blue text; section 2.2). The initial location of each super-individual (black circles) represents the locations of reproductive scallops and the initial number of larvae (red circles) is based on the abundance and fecundity of scallops at that location (details in section 2.3). Settlement is initiated once the larva has grown to the appropriate size. The number of scallops that settle is determined by the number of larvae that remain "in" the super-individual at the time of settlement (see section 2.4).

The simulation program used $\sim$100,000 super-individuals to represent trillions of larvae. Mortality of these larvae was simulated by reducing the number represented by each super-individual as the simulation progressed, such that n was also a function of time. The methods by which interactions between position, size and number of larvae and the simulated environment are described in section 2.2.

The initial positions of super-individuals were chosen to correspond to locations where scallops are observed. These positions were determined by analysis of tow data, which identified three regions were abundance of scallops is high. These regions corresponded to the GSC, NEP and SF subpopulations discussed in chapter 1. Super-individuals were initialized within each of the three regions at the time of spawning. In chapter 3, the transport of super-individuals was examined without reference to the number of larvae represented by each. In chapter 4, the number of larvae represented by a super-individual was based on an estimate of the number of larvae that are spawned at its initial position. The number of larvae spawned at each initial position was estimated by multiplying the number of scallops at that location by their mean fecundity. The distribution and fecundity of scallops were also estimated from tow data. The methods that were used are described

in section 2.3.

The results of the particle-tracking model were analyzed by making plots of the distribution of individuals at the time of settlement, and by counting the number of individuals that were exchanged between the three subpopulations. These methods are described in more detail in section 2.4.

2.1 Environment

The physical environment (the currents, turbulence, temperature and density) on GB was simulated using the Finite-Volume Coastal Ocean Model (FVCOM; *Chen et al.*, 2003). This model was forced with climatological average hydrography at the domain borders and allowed to reach quasi-steady state (*Pringle*, 2006). The hydrographic measurements used to force the model were taken over the years 1970-2003, so the resulting fields reflect the climatological mean circulation and hydrography for that era. Because more measurements were taken in the later years, the resulting hydrodynamics were more representative of conditions in the years between 1990-2003 (*Pringle*, 2006). Following *Johnson et al.* (2006), the modelled currents, temperature, mixing, and water density were averaged using Lagrangian residual quantities, which represent the average value that a passive particle would experience as it is displaced over one tidal cycle (see appendix D for details). Use of Lagrangian residual quantities reduces the amount and dimension of data that need to be stored and indexed, and allows the use of a large time-step in the particle-tracking algorithm ($\Delta t = M_2$ tidal period $= 12.42$ hours). The hydrodynamic model was run for every month, and the Lagrangian quantities were extracted for each run. The resulting fields were taken to represent the physical environment at the temporal middle of each month. The final products were thus monthly-average Lagrangian residual quantities for currents (u, v, w), temperature (T), mixing (k) and density (ρ). The temporal evolution

of these quantities was simulated by linearly interpolating in time between months (see *Johnson et al.*, 2006), allowing an estimate of the fields to be interpolated in time for each model time-step.

2.1.1 Residual Currents

Both spring and fall residual circulation demonstrated the classic GB features: (i) an anti-cyclonic gyre associated with the tidal mixing front roughly along the 60 m isobath, and (ii) fast along-shelf currents on the outer flanks roughly between the 60 and 200m isobaths (*Naimie et al.*, 1994, 2001). Flow in the fall was somewhat faster than in spring (8.4 cm/s vs. 6.7 cm/s), due to seasonal variations in winds, temperatures and stratification. In fall, the anti-cyclonic gyre began strong in September, with water flowing southwest along the southern flank and then tending to recirculate around GB by entering into the GSC, as consistent with other studies of circulation in the area (*Naimie et al.*, 2001). However, the gyre weakened as surface temperatures and stratification decreased, leading to stronger currents flowing to the southwest implying a lower likelihood of retention for water parcels. In spring, the opposite trend occurred: the gyre was weak in early spring, but became stronger as time progressed and summer approached.

2.1.2 Surface Temperatures

Surface temperatures on GB decreased over the fall months (Sept-Nov), and varied spatially (figure 2.2). The NEP was consistently the coldest subregion (15-11 °C), and SF the warmest (18-13 °C). The temperature increase in spring (May-Jul) was more dramatic than the fall decrease with the NEP still representing the coldest subregion (6-14 °C) and SF the warmest (7-18 °C). There was a strong thermocline in fall, with deeper water remaining relatively cooler. The thermocline was very weak in May but became stronger as surface waters warmed going in to summer. This means that there was a larger vertical temperature gradient in fall than in spring, though one was present in both seasons.

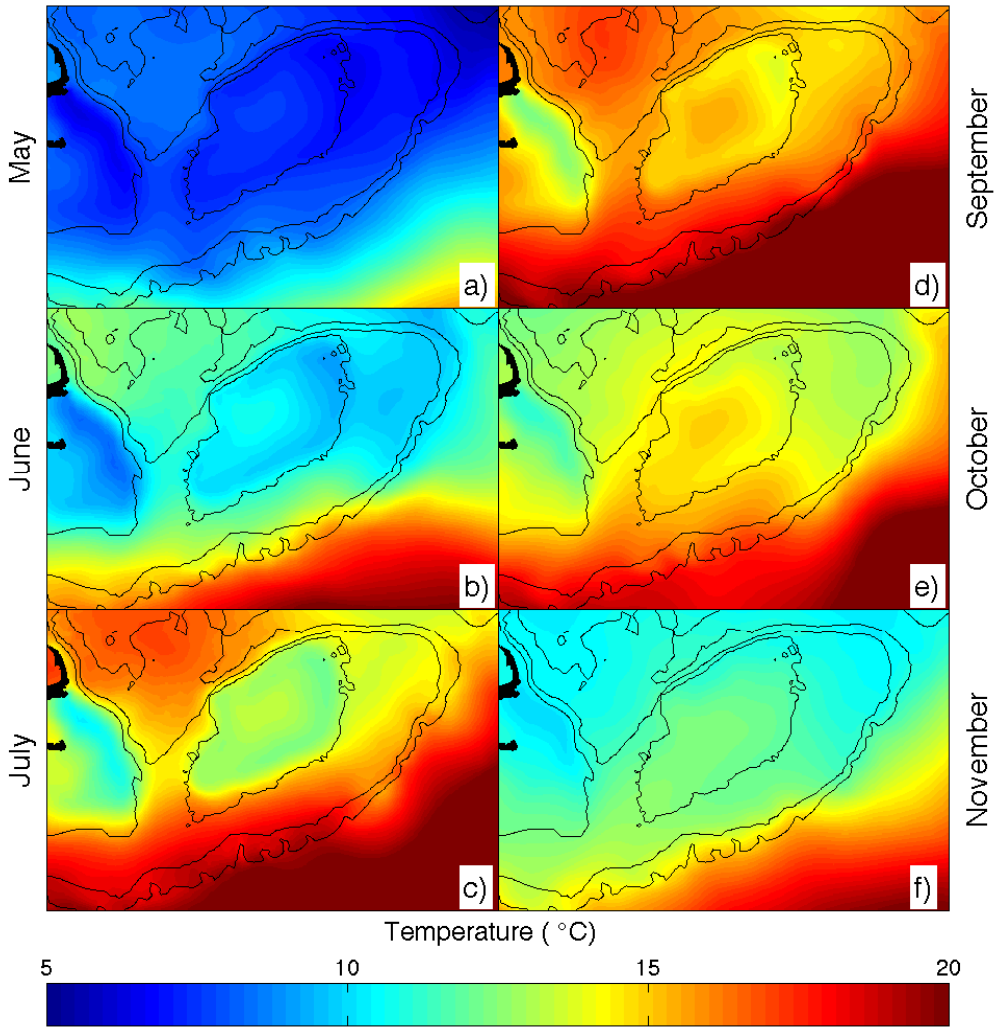

Figure 2.2: Temperature distribution on GB in spring and in fall.

2.1.3 Pycnocline Depths

The pycnocline depth, z_p, was estimated for each horizontal location in the model domain in each month by identifying the depth at which the local density, $\rho(x, y, z_p)$, became higher than the surface density, $\rho(x, y, 0)$, by a threshold value (*Thomson and Fine*, 2003). This value was chosen to be $\Delta\rho = 0.6$ kg m^{-3}, as it leads to estimates of z_p that are consistent with observed pycnocline depths for September (*Tremblay and Sinclair*, 1990; *Tremblay et al.*, 1994). Locations where this threshold was not reached within the upper 40 m of the water-column were considered *well-mixed* and therefore had no pycnocline

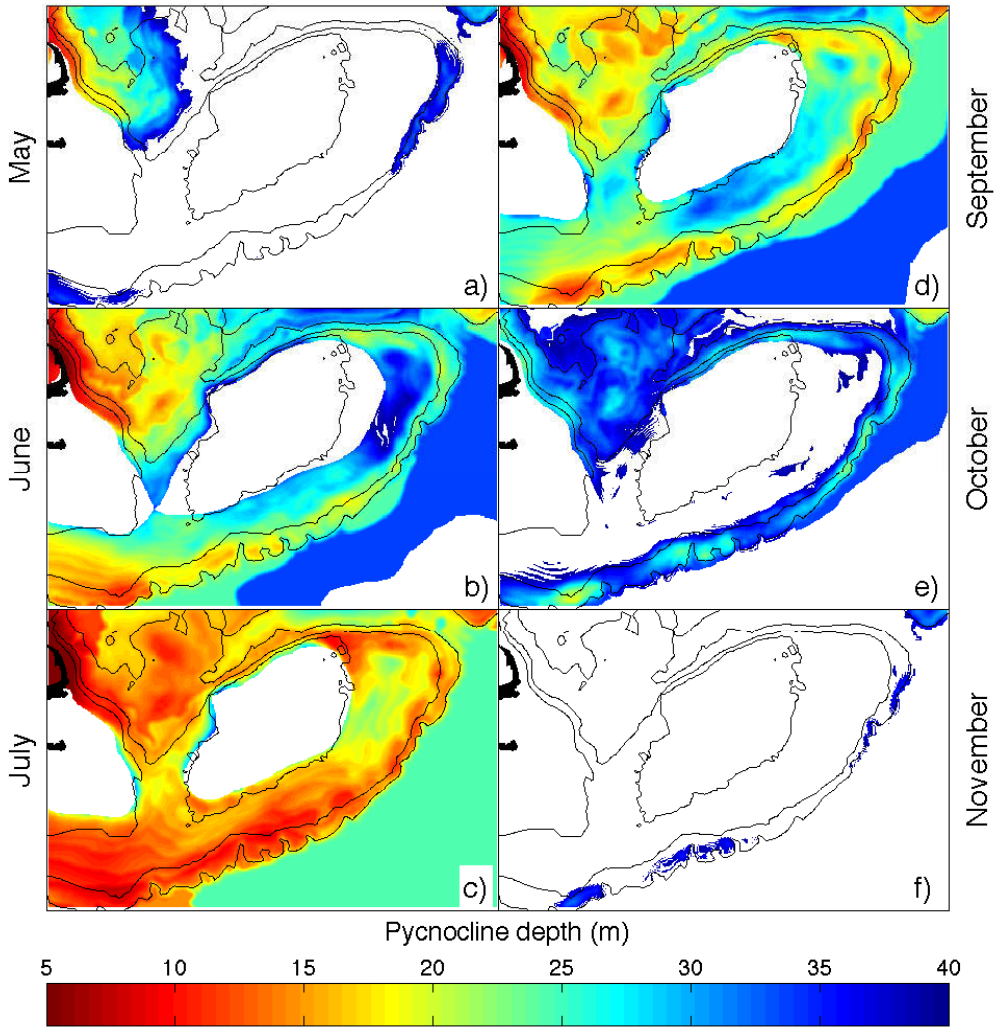

Figure 2.3: Pycnocline depth on GB in spring and fall. White regions denote areas that are *well-mixed*

depth associated with them. Locations at which the pycnocline was successfully identified by this algorithm were considered *stratified*.

The mean pycnocline depth in September was 23 m in both the NEP and GSC and 32 m in the SF, but erosion of the mixed layer over the fall led to all of GB being *well-mixed* by November (figure 2.3). In spring, the opposite trends were observed. GB was *well-mixed* in May, but stratification increased with seasonal warming, such that mean pycnocline depths in July were 10-20 m, with deeper pycnoclines in NEP and GSC than in the SF (figure 2.3).

2.2 Simulating Super-Individuals

2.2.1 Transport

Larval displacement is dependent on currents and larval swimming. Horizontal currents flow at speeds on the order of 1 m s^{-1}, while scallop larvae swim at no more than 1 mm s^{-1} (*Chia et al.*, 1984). This suggests that the contribution of horizontal swimming to horizontal displacement of larvae is negligible. Thus, no horizontal swimming behaviour was simulated and the horizontal displacement of super-individuals over one tidal time-step was computed as:

$$\begin{aligned} x_{ind}^{k+1} &= x_{ind}^{k} + u(x_{ind}^{k}, y_{ind}^{k}, z_{ind}^{k}, t_k)\Delta t \\ y_{ind}^{k+1} &= y_{ind}^{k} + v(x_{ind}^{k}, y_{ind}^{k}, z_{ind}^{k}, t_k)\Delta t. \end{aligned} \tag{2.1}$$

Terms of the form x_{ind}^{k} are short-hand for $x_{ind}(t_k)$ and terms of the form x_{ind}^{k+1} are short for $x_{ind}(t_k + \Delta t)$. This notation is used here to make the equations in this section more readable. The ordered pair (x_{ind}, y_{ind}) refers to the horizontal location of one individual, and the terms (u, v) are the Lagrangian residual velocities.

Vertical current velocities are on the same order of magnitude as swimming velocities and therefore might be overcome by larval swimming. Thus, different assumptions about the vertical swimming behaviour of larvae were contrasted. Larval swimming behaviour and ability change with larval stage and size (*Culliney*, 1974; *Chia et al.*, 1984; *Tremblay et al.*, 1994). The larvae progress through the trochophore, veliger and pediveliger stages before settling and each of these phases is associated with a particular swimming behaviour (see appendix A for details). However, the veliger phase is by far the longest of the planktonic phases ($\sim$30 d in fall), while the total duration of the other phases combined may be as short as $\sim$5 d in total. In the interest of simplicity, behaviours associated with trochophores and pediveligers were not simulated. Instead, the swimming behaviour

associated with veliger larvae was simulated over the entire 35 d planktonic duration. The vertical behaviour of veliger larvae was simulated separately for two contrasting behavioural assumptions, hereafter referred to as *passive* and *pycnocline-seeking*.

It is unknown whether scallops can extend their planktonic existence to search the bottom for suitable settlement habitat. Such a behaviour has the potential to affect dispersal if it exists, but it was not simulated as so little is known about it. If this phase is discovered to have significant impact on dispersal, some of the results in this thesis will have to be reinterpreted as showing the distribution of larvae at the beginning of settlement, not at the final position of the scallops.

Larvae exhibiting *passive* behaviour did not swim, and so were transported by vertical currents and turbulence. The vertical displacement over one time-step was computed as

$$z_{ind}^{k+1} = z_{ind}^{k} + w(x_{ind}^{k}, y_{ind}^{k}, z_{ind}^{k}, t_k)\Delta t + \Delta z_{turb}^{k} \tag{2.2}$$

where w is the vertical Lagrangian residual velocity, and Δz_{turb} is a random walk based on the local value of the turbulent mixing coefficient, $k(x_{ind}, y_{ind}, z_{ind}, t_k)$. The random walk was calculated using an algorithm with a small time step, $d\tau \ll \Delta t$, in order to avoid unrealistic accumulation of individuals at depths with low mixing (*Visser*, 1997). *Visser* (1997) recommends use of a time-step that is much smaller than the second-order derivative of k in the vertical direction, such that

$$d\tau \ll \left(\frac{\partial^2 k}{\partial z^2}\right)^{-1} \tag{2.3}$$

for all points in the domain. Choosing $d\tau$ =75 s satisfied this criterion over most of the model domain, except for some shallow highly-mixed regions where the required time step was computationally prohibitive (i.e. $d\tau \ll$1 s). For particles in these select regions, an alternative approach was used in which $z_{ind}(t + \Delta t)$ was randomly sampled from a

uniform distribution of depths within the water column. This strategy led to proper larval distributions because mixing in these regions was high enough and water-column depth was low enough that larvae could be displaced in excess of the watch-column depth within one model time-step, Δt. Observed larval distributions in *well-mixed* regions also match this type of distribution (*Tremblay and Sinclair*, 1990), suggesting that this method is appropriate.

The *pycnocline-seeking* behaviour was designed to reflect observations that *P. magellanicus* larvae are aggregated at the pycnocline in stratified regions and distributed within the water-column in well-mixed regions (*Tremblay and Sinclair*, 1990). Hence, modelled vertical displacement was conditional on the presence or lack of a pycnocline. Individual depths were computed as:

$$z_{ind}^{k+1} = \begin{cases} z_p(x_{ind}^{k+1}, y_{ind}^{k+1}, t_k) & \text{if } \textit{stratified} \\ z_{ind}^{k} + w(x_{ind}^{k}, y_{ind}^{k}, z_{ind}^{k}, t_k)\Delta t + \Delta z_{turb}^{k} & \text{if } \textit{well-mixed} \\ d(x_{ind}^{k+1}, y_{ind}^{k+1}) R_{ind}^{k+1} & \text{if } d\tau < 75 \text{ s}, \end{cases} \tag{2.4}$$

where z_p is the depth of the pycnocline, d is the depth of the water-column and R is a uniformly distributed random number between zero and 1.

2.2.2 Growth and PLD

Modelled PLD was based on assumptions about how long it takes larvae to grow to their size at settlement, approximately 240-300 µm (*Tremblay et al.*, 1994). At typical fall temperatures (i.e. 12-15 °C), growth rates are 5-6 µmd^{-1} and the corresponding larval development time is 30-40 d (*Tremblay et al.*, 1994). Larval growth rate was assumed to increase exponentially with temperature, such that a change of 10 °C would lead to a doubling in the growth rate (that is, $Q_{10} = 2$). Though the relationship between temperature and growth rate has not been measured for *P. magellanicus*, this relationship has been

observed in the related scallop species, *Pecten maximus* (*Beaumont and Barnes*, 1992). For an ambient temperature $T^k_{ind} = T(x^k_{ind}, y^k_{ind}, z^k_{ind}, t_k)$, the change in the individual's size s_{ind} (µm) over the time step Δt was computed as

$$s_{ind}(t_{k+1}) = s_{ind}(t_k) + g_{ind}(T^k_{ind})\Delta t \ \text{ µm} \tag{2.5}$$

where the individual's growth rate is

$$g_{ind}(T_{ind}) = \begin{cases} 5.7 & \text{µm d}^{-1} \quad \text{if PLD is constant} \\ 5.7Q_{10}^{(T^k_{ind}-13.5)/10} & \text{µm d}^{-1} \quad \text{if PLD is temperature-dependent.} \end{cases}$$

The PLD was taken to be the the time in which an individual grew from its initial size of 70 µm, to a final size of 270 µm. These parameter values were chosen such that the PLD of an individual experiencing typical fall temperatures of 13.5 °C would be 35 d.

2.2.3 Mortality Rate

The death of meroplankton such as scallop larvae is typically attributed to biotic factors such as predation and starvation as well as abiotic factors that lead to physiological stress, such as temperature or salinity (*Metaxas and Saunders*, 2009). The biotic and abiotic environment on GB changes seasonally (zooplankton: *Davis* (1987), phytoplankton: *O'Reilly and Zetlin* (1998), hydrography: *Ashjian et al.* (2001)), so mortality rates for scallop larvae likely differ between the two seasons. A meta-analysis identified a positive correlation between temperature and mortality rates across 23 different taxa *Houde* (1989). *Houde and Bartsch* (2008) suggest that in the absence of species-specific data on the relationship between temperature and mortality, a relationship between the two should be assumed. Since no data on larval mortality rates are available for *P. magellanicus*, the rates were simulated by linking them to temperature via an exponential (Q_{10}) relationship,

wherein the mortality rate $m(T)$ is

$$m(T) = m_0 Q_{10}^{(T-T_0)/10}, \tag{2.6}$$

m_0 is a base mortality rate and T_0 is the reference temperature, chosen to be the same (13.5 °C) as above. The base mortality rate was chosen to be 20 $\%$ d^{-1}. The number of larvae represented by a super-individual at time t_{k+1} was therefore determined by the equation

$$n_{ind}(t_{k+1}) = n_{ind}(t_k) e^{-m(T^k_{ind})\Delta t}. \tag{2.7}$$

Since there are no data to support a specific choice for the Q_{10} factor, two assumptions were contrasted: (1) $Q_{10} = 1$, chosen to illustrate the outcome if larval mortality rates are the same across seasons and (2) $Q_{10} = 2$, chosen to illustrate the outcome if larval survivorship to settlement size is approximately the same in each season. The second option simulates equal survivorship between seasons, because the simulated mortality rate is linked to temperature in the same way as the PLD, so the effect of extending the PLD will be approximately cancelled by the effect of reducing mortality rate. These two assumptions about mortality rates are intended to be illustrative, and do not necessarily reflect the true seasonal difference in mortality rates. The goal is to simply illustrate the effect that plausible inter-seasonal differences in the mortality have on larval connectivity, without the need to explicitly model the mechanisms that cause these changes.

2.3 Larval Production Fields

Scallops on GB form three major aggregations. In this section, the methods by which the geographic extents of these three aggregations were defined is described. The density of

Size-class	**Small**	**Medium**	**Large**
Shell height	50-95 mm	95-120 mm	120-170 mm
Approx. age	2-4 years	4-6 years	>6 years
Fecundity (Spring)	21 M	33 M	61 M
Fecundity (Fall)	36 M	68 M	132 M
Portion (*pre-closures*)	69 %	27 %	4 %
Portion (*post-closures*)	47%	35%	18%

Table 2.1: The three scallop size-classes and their respective specific fecundities.

newly spawned larvae at a given location within these regions depends on the local density of adult female scallops and the average number of larvae that they spawn. Fecundity, taken here to be the number of larvae spawned per female scallop per season, is correlated with scallop size (*Langton et al.*, 1987) and the size-structure of scallop populations may vary in time and space. Thus, the distribution and fecundity of female scallops were both estimated for three different size-classes of scallop hereafter referred to as *small scallops*, *medium scallops* and *large scallops* respectively. Scallops were assigned to these size-classes based on reported shell heights, with small scallops having shell heights between 50 and 95 mm, medium scallops between 95 and 120 mm and large scallops between 120 and 170 mm. Estimates of fecundity (f_{size}) and distribution ($c_{\text{size}}(x, y)$) for scallops in each of these size-classes allowed estimates of the *larval production fields* $l(x, y)$, which describe the density of scallop larval spawned in a particular scallop subpopulation, season, and fishery era as a function of space:

$$l(x, y) = f_{\text{small}} c_{\text{small}}(x, y) + f_{\text{medium}} c_{\text{medium}}(x, y) + f_{\text{large}} c_{\text{large}}(x, y). \tag{2.8}$$

2.3.1 Identifying the Subpopulations

The geographic extents of the three GB subpopulations were delineated by analysis of scallop fishery tow data provided by the Department of Fisheries and Oceans (DFO), Canada and the National Oceanic and Atmospheric Administration (NOAA), United States. Contours of non-negligible scallop density (i.e. > 25 scallops per standardized tow) were computed, identifying two continuous regions: one in the Great South Channel (GSC, figure 1.2), and one on eastern GB. The large eastern region was subdivided into two subregions to correspond to the Northeast Peak (NEP) and the Southern Flank (SF) (figure 1.2). This distinction was made in order to separate the Canadian and U.S. economic zones along the International Court of Justice (ICJ) line, and to be consistent with previous delineations of these subpopulations (*Tremblay et al.*, 1994).

The GSC subpopulation as estimated from this procedure has an area of 2,500 km^2. The middle of the bed over the deepest part of the channel contains very few scallops (Hart, pers comm.). This small segment was not counted as a part of the bed in chapter 4. The NEP subpopulation fills an area of 2,100 km^2 and covers the entire Canadian portion of GB to a depth of 120 m, as well as a small part in US waters along the northern flank where scallop density is very high. The SF subpopulation has an area of 1,800 km^2 and runs along the southern flank of GB, mostly between the 60m and 100m isobaths (figure 1.2). These subpopulations are located in the same general regions as in previous models (*Tremblay et al.*, 1994), but their geographic extents are not exactly the same. The GSC extends farther to the north and to the south, the NEP is similar and the SF is much larger here than in previous models, extending further to the southwest. All areas outside of these beds were considered to be unsuitable habitat (UH) for scallops to settle and then survive to recruitment age. The lack of scallops in these regions suggests that any larvae attempting to settle in these regions experience high mortality rates during or shortly after settlement.

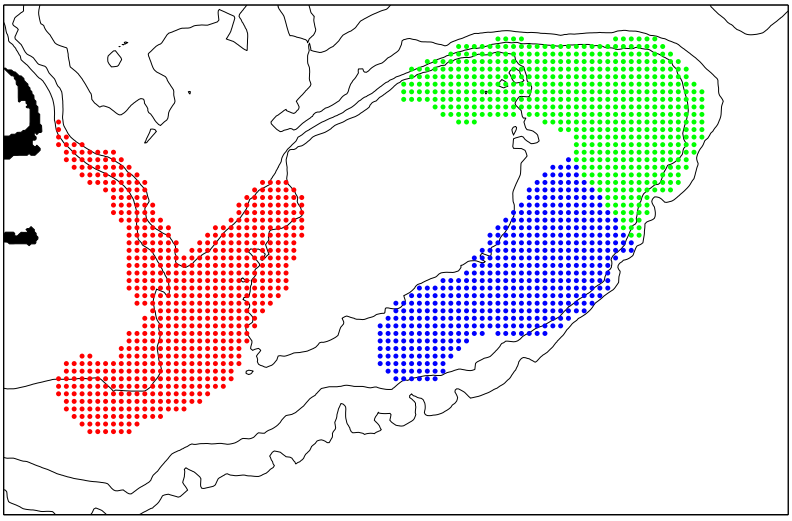

Figure 2.4: The initial positions for super-individuals. Sixty-four super-individuals are initialized at each point in this grid.

The geographic definitions of the subpopulations were used to select suitable initial positions for super-individuals. A 4 km by 4 km grid was defined within each subpopulation (see figure 2.4), and 64 super-individuals were initialized at each of those points. In all, 30,000-40,000 super-individuals were initialized in each subpopulation.

2.3.2 Scallop Abundance & Distributon

The distribution of female scallops was characterized by estimating the density of scallops in each size-class in each subpopulation as a function of space, $c_{\text{size}}(x, y)$. The density estimates were based on fishery tow data provided by DFO and NOAA. All records of scallop abundance were standardized and amalgamated and then sorted into eighteen different subsets, according to size-class (small, medium, large), subpopulation (GSC, NEP, SF) and fishery era (*pre-closures*, *post-closures*). In each case, the density of scallops was estimated using a kriging procedure and then divided by two to give the density of females, under the assumption of an equal sex ratio.

Data records reporting a density of 0 scallops m^{-1} were added to the data sets at the bed borders so as to ensure that estimated scallop density was zero near these borders, as

indicated by observations. The same was done for the gap in the middle of the GSC, where few scallops are observed to exist (*D. Hart, personal communication*). Scallop abundance per tow was transformed as $\log(\text{abundance}+1)$, as the frequency distribution of abundance per tow was better fit by a log-normal distribution than by a normal distribution. This is consistent with other attempts to estimate scallop distribution by kriging, in which it was also found that scallop density is best modelled as a log-normally distributed random variable (*Ecker and Heltsche*, 1994). For simplicity, the variogram was chosen to be exponential and isotropic. Though *Adams et al.* (2008) recommend de-trending and correcting for anisotropy when kriging scallop distribution, this was not done here. The autocorrelation in scallop density is likely anisotropic, with correlation higher in the along-isobath direction. But because the isobaths change direction within the subpopulations, this makes a correction for anisotropy difficult. Variograms were estimated empirically from the data for each bed and then used to krige scallop density at each super-individual's initial-position. This was done in R by using the "krige" command from the package "geoR" (*Ribeiro Jr and Diggle*, 2001).

Subjective comparison of raw data with the kriges suggests that the most important characteristics of the distribution of scallops were captured. For example, a bubble plot of the density of small scallops reported in the tow data and a plot of the corresponding kriged density look very similar (figure 2.5). The results of this procedure for other size-classes, beds and eras are not shown directly in this thesis, but the larval production fields that they are used to estimate are shown and discussed in chapter 4.

2.3.3 Size-Specific Fecundity

The seasonal size-specific fecundity f was estimated from female scallop gonad data collected on the NEP over the years 1984-2004 (*DFO; unpublished data*). Monthly averages of measured wet gonad weight (WGW) were computed for each year, creating a

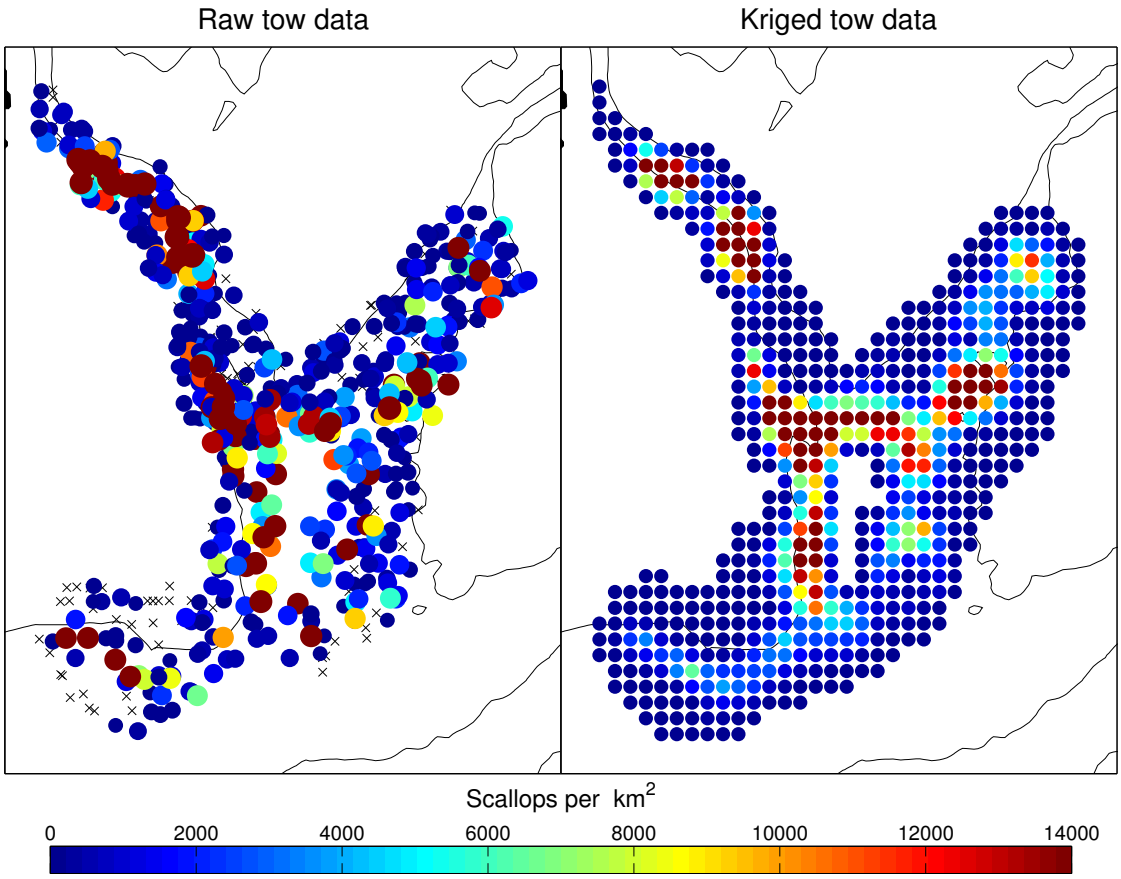

Figure 2.5: Comparison between standardized scallop tow data and kriged scallop density in the GSC. The distribution of small scallops is shown.

sampled time-series. Each annual times-series was analyzed, with any decrease in WGW occurring between the months of February and June (inclusive) taken to indicate spring spawning activity, and any decrease occurring between the months of July and November as fall spawning. The total decrease in WGW was recorded for each season in each year. There were not enough data collected in 1998 to infer the presence or lack of spawning in either season, so results for this year were excluded from the analysis. In some years there were not enough large scallops sampled in order to estimate a reliable monthly mean gonad weight. In these years, no estimate of spawning output for large scallops was made. The seasonal drops in WGW were used to estimate the number of eggs produced by dividing this drop by the typical mass of an egg (1.6×10^{-7} g; *Langton et al.*, 1987). The drop in WGW after spring spawning may be obscured because spring spawners return immediately

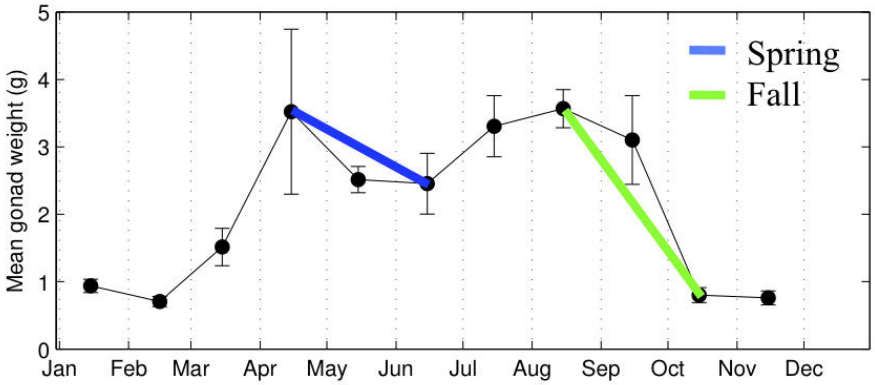

Figure 2.6: Monthly averaged gonad weight of small (50-95 mm) female scallops in 1990. The drop in the mean weight in spring (blue line) is teaken to represent spring spawning, and the drop during the fall (green line) is taken to represent fall spawning.

to producing more gametes (*DiBacco et al.*, 1995). This means that the estimates of spring spawning magnitude are conservative, and that true spring fecundity may be higher. The estimates for each size-class in each season are shown in table 2.1.

2.4 Summarizing Simulated Larval Dispersal and Connectivity

The individual-based particle-tracking model was run under different assumptions. In chapter 3, each simulation required assumptions about

1. **swimming behaviour**: either *passive* or *pycnocline-seeking*
2. **temperature effects on PLD**: either *constant* or *temperature-dependent*
3. **spawning season**: either spring or fall.

The position of each particle at the end of its simulated PLD was taken to be its *settlement position*, keeping in mind that in reality this position may be affected by unmodelled settlement processes that occur after the veliger phase. The *settlement distribution* of super-individuals was plotted for various combinations of the model assumptions listed

above, allowing a detailed analysis of the effects of each factor on dispersal. In chapter 3, the number of larvae represented by each super-individual was not considered. Only the dispersal of super-individuals was investigated. Since these super-individuals only represent one hypothetical individual each, they are referred to "particles" in the following chapter.

The exchange of super-individuals among the 3 subpopulations, the *transport connectivity*, was summarized by defining a *connection fraction*, $\phi_{(i,j)}$, which equals the fraction of particles "spawned" in subpopulation j (where j is GSC, NEP, or SF) that settled in region i, where i can be one of the three subpopulations as well as "unsuitable habitat" (UH) or "downstream" (DS). The DS region was defined as all locations west of 71°W and represents potential supply to scallop populations southwest of GB, such as the Mid-Atlantic Bight. UH was defined as any region outside of the subpopulations and upstream (east) of DS, which correspond to locations where no significant scallop densities are observed (*Hart and Chute*, 2004) and thus where the benthic substrate is assumed to be uninhabitable. Connection fractions were summarized in a transport connectivity matrix,

$$\mathbf{\Phi} = \begin{pmatrix} \phi_{GSC,GSC} & \phi_{GSC,NEP} & \phi_{GSC,SF} \\ \phi_{NEP,GSC} & \phi_{NEP,NEP} & \phi_{NEP,SF} \\ \phi_{SF,GSC} & \phi_{SF,NEP} & \phi_{SF,SF} \\ \phi_{UH,GSC} & \phi_{UH,NEP} & \phi_{UH,SF} \\ \phi_{DS,GSC} & \phi_{DS,NEP} & \phi_{DS,SF} \end{pmatrix}. \tag{2.9}$$

In chapter 4, assumptions about swimming behaviour (*pycnocline-seeking*) and temperature-effects on PLD (individually varying) were made, allowing focus to be put on the impact of demographic factors on larval dispersal. To test these, varying assumptions were made about:

1. **the larval production field**: either *homogeneous* or *heterogeneous*

2. **temperature effects on mortality**: either *constant* or *temperature-dependent*.

Then, as a case study, simulated *larval connectivity* for the *post-closures heterogeneous* larval production field was compared with that for the *pre-closures heterogeneous* larval production field. In chapter 4, each super-individual was taken to represent a particular number of larvae. At the beginning of each simulation, the local value of the larval production field was multiplied by 16 km^2 to give the abundance of larvae spawned in the vicinity and divided equally among all 64 super-individuals spawned at that point. Mortality was then simulated over the PLD, and that number of larvae remaining "in" the super-individual were counted at settlement.

The exchange of simulated larvae among subpopulations was quantified by tabulating the number, $\ell_{(i,j)}$, of larvae spawned by subpopulation j that settled in subpopulation i. It was convenient to give these numbers a general name, so they are referred to as *migration rates* in this thesis. This is an operational definition and the word simply refers to one number, ℓ. The number of larvae being transported to DS habitat was not recorded in these simulations because mortality could not be simulated once super-individuals left the domain. The larval connectivity matrix was computed as

$$\mathbf{L} = \begin{pmatrix} \ell_{GSC,GSC} & \ell_{GSC,NEP} & \ell_{GSC,SF} \\ \ell_{NEP,GSC} & \ell_{NEP,NEP} & \ell_{NEP,SF} \\ \ell_{SF,GSC} & \ell_{SF,NEP} & \ell_{SF,SF} \\ \ell_{UH,GSC} & \ell_{UH,NEP} & \ell_{UH,SF} \end{pmatrix}. \tag{2.10}$$

CHAPTER 3

BIOLOGICAL FACTORS INFLUENCING LARVAL DISPERSAL

The results in this chapter are also published in:

Gilbert, C., W. Gentleman, C. Johnson, C. DiBacco, J. Pringle, and C. Chen, Modelling dispersal of sea scallop (*Placopecten magellanicus*) larvae on Georges Bank: The influence of depth distribution, planktonic duration and spawning seasonality, *Progress In Oceanography*, 87, 37-48, 2010.

In this chapter, the particle-tracking model described in chapter 2 is used to quantify the influence of biological factors on the dispersal of *P. magellanicus* larvae on GB. Specifically, the interactions of climatological circulation and hydrography with variations in (1) depth distribution, (2) temperature-dependent PLD, and (3) spawning season are simulated in order to observe their effect on larval transport. By assessing the extent to which these factors affect retention and exchange among GB subpopulations, this work provides insight into the biophysical processes governing population connectivity in *P. magellanicus* on GB, and helps direct future research programs by identifying the kinds of data needed to improve our ability to model and understand the relationship between these three subpopulations.

3.1 Results

3.1.1 Effect of Swimming Behaviour on Dispersal

Simulated transport of larvae with a temperature-independent PLD of 35 d and *passive* swimming behaviour supported findings from previous studies that used similar assumptions. These studies all indicate significant drift among the three subpopulations (figure 3.1a-c; table 3.1; *Tremblay et al.*, 1994; *Tian et al.*, 2009a). Thirty-nine percent of particles spawned in the GSC were transported DS, and 24 % settled in UH, leaving 37 % remaining within the metapopulation. GSC-spawned particles were locally retained at approximately the same rate they settled in the other two subpopulations combined (20 % vs. 17 %). In contrast, virtually no NEP-spawned particles left GB or were locally retained (figure 3.1b), and instead the majority settled in UH (61 %, table 3.1, figure 3.1b). The proportion of NEP-spawned particles retained within the metapopulation was 39 % – effectively the same as the GSC – and they settled in both the SF (22%) and GSC (13 %). Thirty-seven percent of particles spawned in the SF settled in UH, and another 14 % were lost to DS. Like those from the NEP, local retention of SF-spawned particles was negligible; most were transported to the GSC (45 %, table 3.1, figure 3.1c).

In the preceding simulation, particles were initialized at the local pycnocline in September, so as to be consistent with observations and previous model investigations (*Tremblay et al.*, 1994; *Tian et al.*, 2009a). However, particle depths quickly became uncorrelated with the pycnocline (figure 3.2). This de-correlation was due in part to large random-walk excursions ($\Delta z > 20$ m per tidal period) resulting from mixing, and in part to the seasonal deepening of the pycnocline as the simulation progressed. By the end of the simulation, more than a third of the particles were more than 20 m from the pycnocline. Thus, the depth distribution resulting from *passive* behaviour is inconsistent with observations (*Tremblay and Sinclair*, 1990). In order to remain in the pycnocline, larvae would need to overcome

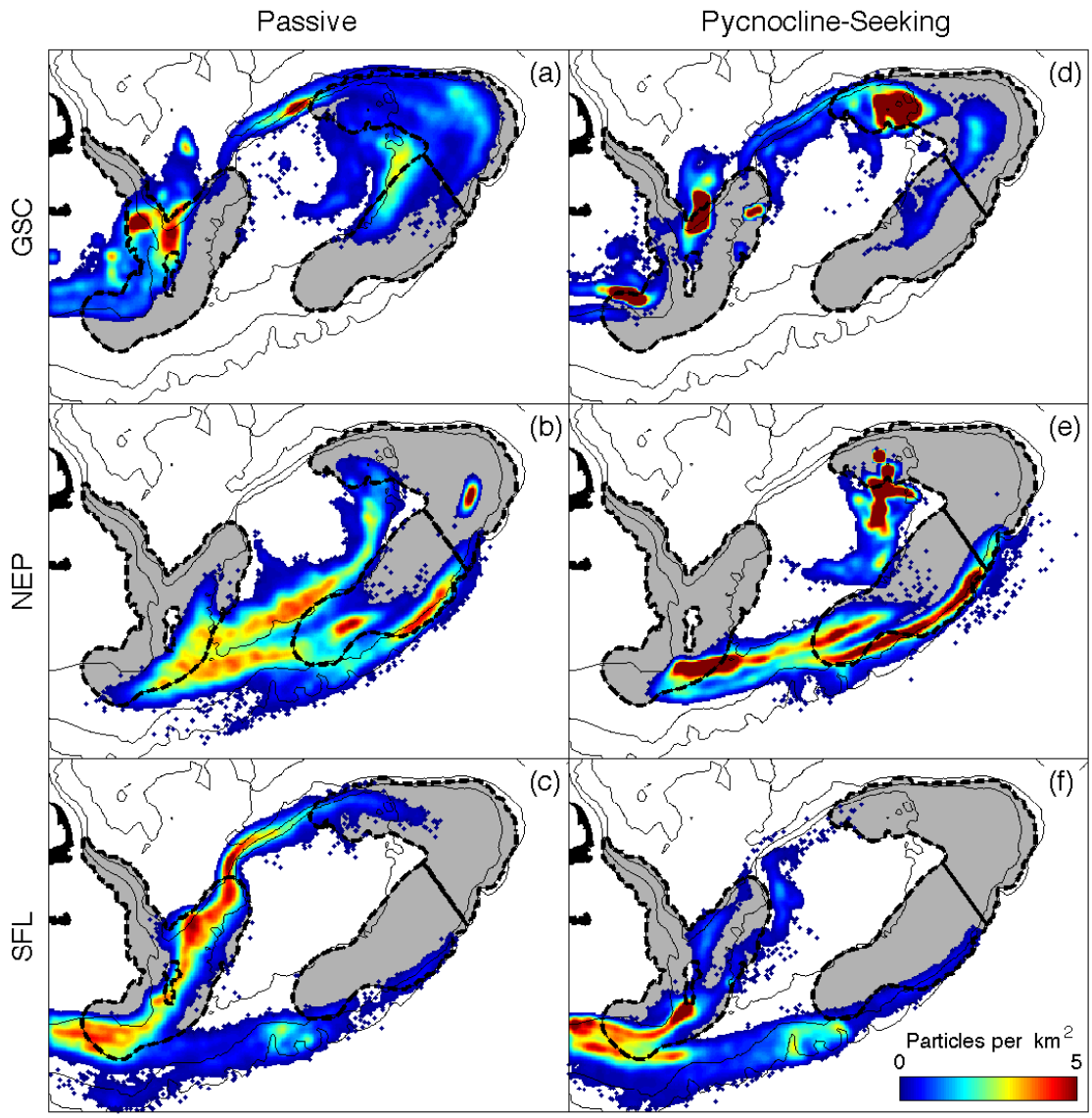

Figure 3.1: Particle distribution after 35 d in fall for both the *passive* and *pycnocline-seeking* behaviours. The distributions for the GSC-spawned (a and d), NEP-spawned (b and e), and SF-spawned (c and f) particles are each shown separately.

net advective and dispersive displacements of $\sim$20 m over a tidal cycle, which corresponds to mean vertical swimming speeds of $\sim$0.4 mms^{-1}. This is within the range of capabilities of *P. magellanicus* larvae reported in the literature (*Chia et al.*, 1984; *Tremblay et al.*, 1994).

To assess how a more realistic larval depth distribution influences larval drift, the transport of *pycnocline-seeking* particles was modelled. Results for simulations using constant

Description	Settlement Region	Passive Spawning GSC	Passive Spawning NEP	Passive Spawning SF	Pycnocline-seeking Spawning GSC	Pycnocline-seeking Spawning NEP	Pycnocline-seeking Spawning SF
Fraction Settling							
	GSC	20	13	45	21	12	22
1.	NEP	12	4	3	35	8	0
Fall	SF	5	22	1	1	28	1
PLD_0	UH	24	61	37	18	52	14
	DS	39	0	14	35	0	63
	GSC	18	15	47	21	13	25
2.	NEP	13	4	4	24	7	0
Fall	SF	8	16	1	2	23	1
$PLD(T)$	UH	21	65	36	18	56	43
	DS	40	0	12	35	0	31
	GSC	4	23	24	18	0	7
3.	NEP	8	4	4	13	14	1
Spring	SF	7	9	0	1	5	0
$PLD(T)$	UH	22	63	23	17	81	51
	DS	59	1	49	51	0	41

Table 3.1: Particle connectivity matrices summarizing model simulation results for six different model scenarios. *Passive* and *pycnocline-seeking* behaviours are compared for the fall, with a *constant* PLD (row 1), fall with *temperature-dependent* PLD (row 2), and spring, with a *temperature-dependent* PLD (row 3).

growth rates are shown in figure 3.1d-f and table 3.1. Overall retention within the metapopulation was similar for *pycnocline-seeking* and *passive* behaviours, but there were some pronounced changes in settlement distributions and the amount of exchange occurring among subpopulations. Connection fractions for GSC-spawned *pycnocline-seeking* particles were not substantially different from the *passive* case, with the notable exception of settlement in the NEP, which doubled (25 % vs. 12 %) due to the dense aggregation of particles settling inside of the 60 m isobath (figure 3.1d). While settlement distributions for NEP-spawned *pycnocline-seeking* particles were more densely aggregated (figure 3.1e vs. 4b), connection fractions were essentially unchanged from the *passive* case. Loss of SF-spawned *pycnocline-seeking* particles to DS increased dramatically relative to the *passive* case (63 % vs. 14 %), due to most particles now being transported in the along-shelf currents. This increase in transport to DS altered the settlement distribution of SF-spawned

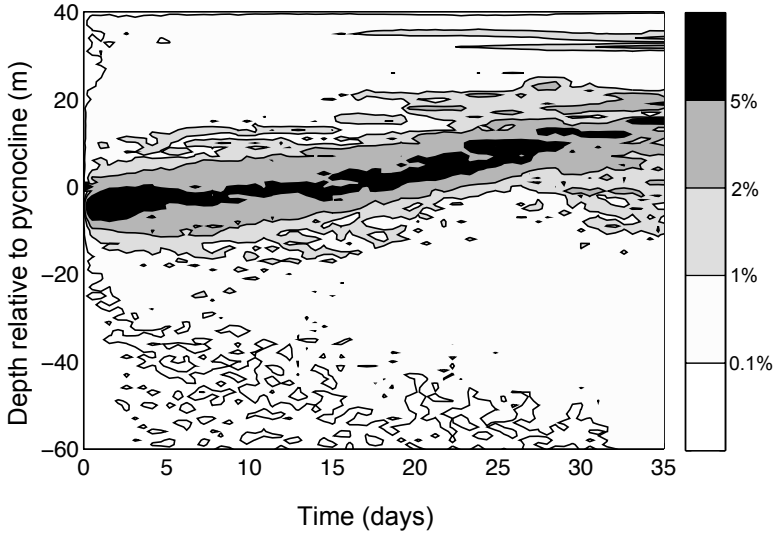

Figure 3.2: Depth distribution of *passive* particles relative to the pycnocline.

pycnocline-seeking particles (figure 3.1c vs. 4f), and reduced the fraction settling in the GSC (22 % vs. 45 %) and in UH (14 % vs. 37 %).

3.1.2 Effect of Temperature-dependent growth on Dispersal

The particle-tracking simulation a was re-run with temperature-dependent growth (see subsection **??**). Variation in the fall temperature fields led to a range of PLDs that was similar to previous estimates (i.e. figure 3.3 vs. 30-40 d: *Tremblay et al.*, 1994). This range was larger for *passive* than for *pycnocline-seeking* particles (30-54 d *passive* vs. 27-43 d *pycnocline-seeking*), due to their broader distribution across vertical temperature gradients. The mean fall PLD was 37 d for *passive* and 36 d for *pycnocline-seeking* behaviours, indicating that the average temperature along the particle paths was slightly lower than 13.5 °C for which PLD = 35 d. The longer PLD associated with the *passive* simulation was due to a greater proportion of particles being distributed in the colder waters below the thermocline.

The mean temperature near the pycnocline in spring is ∼9.5 °C, which corresponds to a mean PLD of 48 days (for $Q_{10} = 2$) – almost two weeks longer than the mean PLD in fall.

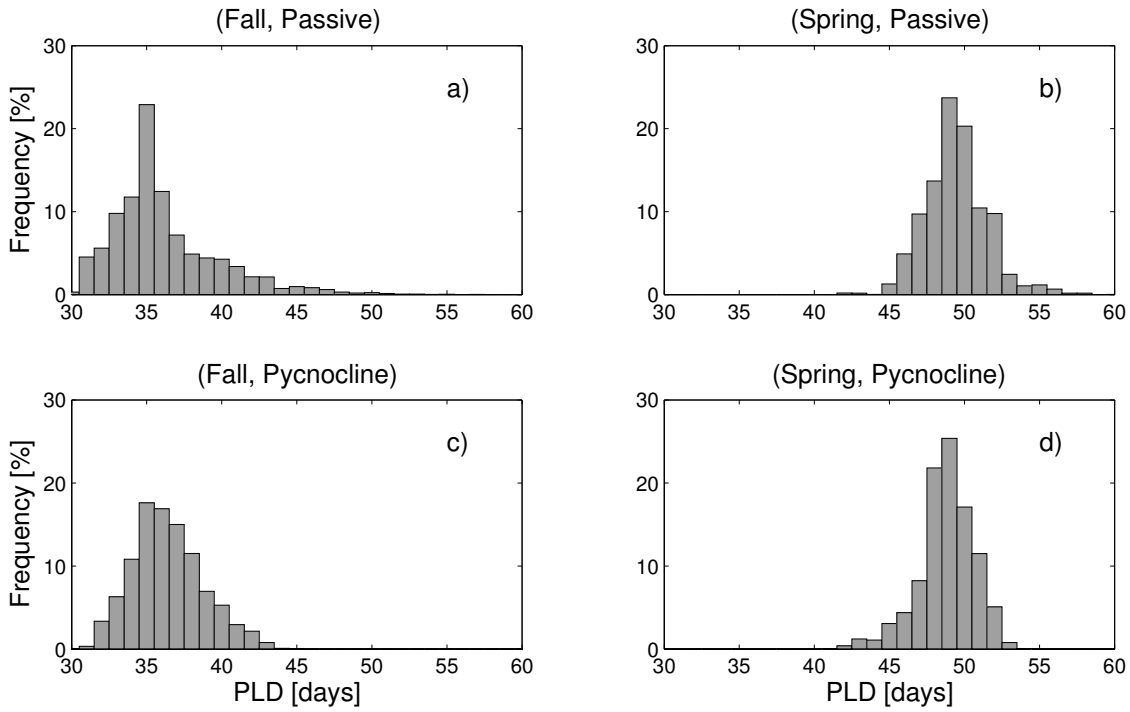

Figure 3.3: Frequency distribution of PLDs for particles with temperature-dependent growth rates.

Spring simulations using temperature-dependent growth also resulted in a wide range of PLDs (40-60 d *passive* vs. 39-53 d *pycnocline-seeking*). The mean spring PLD was 49 d for *passive* and 47 d for *pycnocline-seeking* particles, indicating the average temperature along their paths was $\sim$9.5 °C. There were no substantial differences in predicted dispersal for fall simulations with constant growth rate from those with temperature-dependent growth (figure 3.4 vs. figure 3.1; table 3.1). The only exception was for *pycnocline-seeking* particles spawned in the SF, for which temperature-dependent growth reduced the fraction of articles lost to DS (63% vs. 31%) and increased the fraction settling in UH (14 % vs. 43 %). These changes were due to accelerated growth in the warm southern flank slope waters and resulted in more particles reaching settlement size before they could be advected out of the domain. Spring simulations exhibited the same lack of sensitivity as seen in fall, such that results for temperature dependent growth (figure 3.5) were effectively the same as those for a constant PLD of 48 d (*not shown*). Hence, all results discussed in the following section are for the temperature-dependent case.

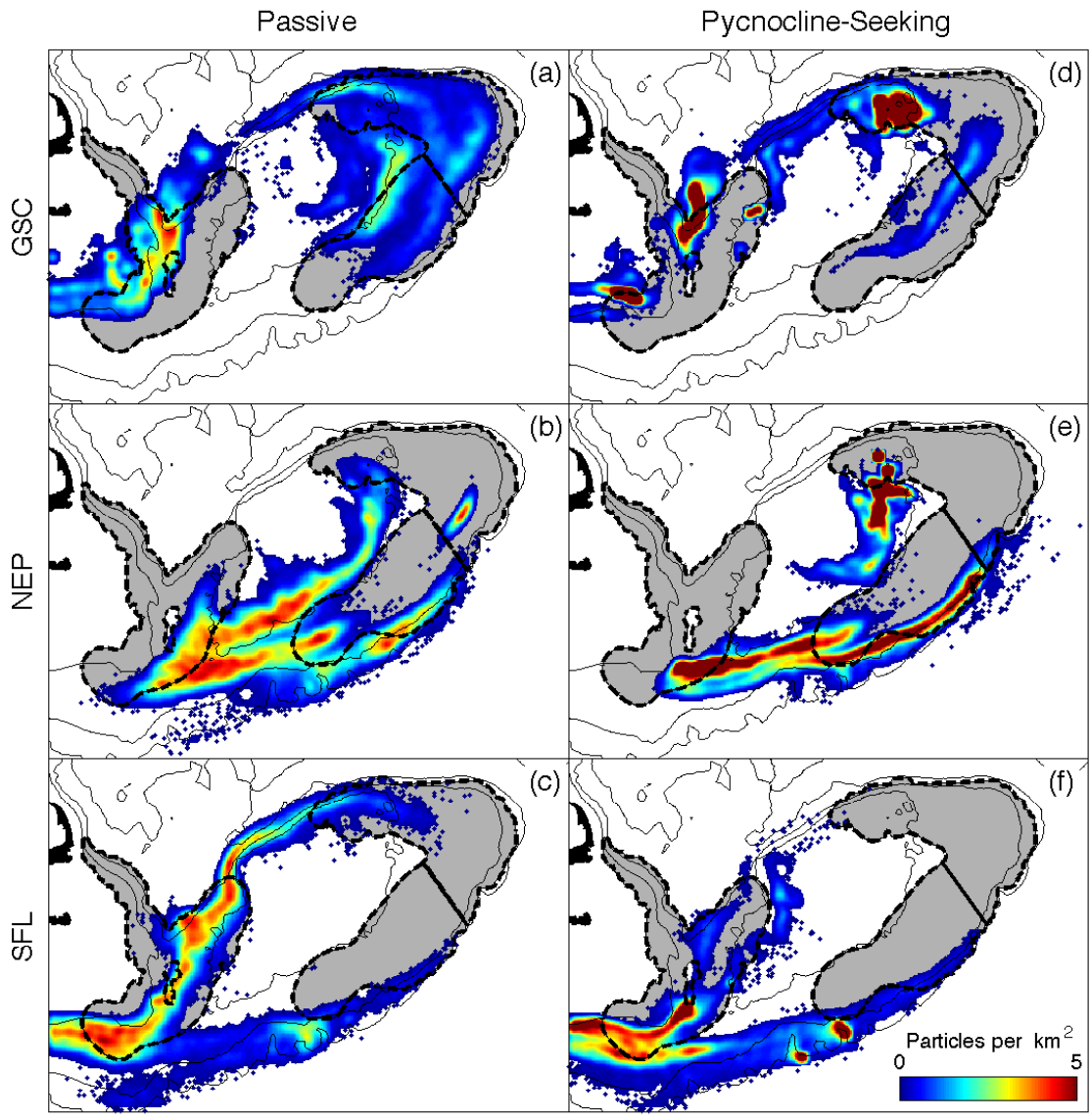

Figure 3.4: Particle distribution in fall for both the *passive* and *pycnocline-seeking* behaviours, with temperature-dependent PLD. The distributions for the GSC-spawned (a and d), NEP-spawned (b and e), and SF-spawned (c and f) particles are each shown separately.

3.1.3 Effect of Spawning Season on Dispersal

Settlement distributions for larvae with temperature-dependent growth rate and *passive* behaviour were similar in both the spring and fall (figure 3.4a-c vs. figure 3.5a-c), indicating that longer spring PLDs coincidentally balanced slower spring currents. However, there were several noteworthy differences in rates of exchange among the subpopulations (table 3.1). For GSC-spawned particles in spring, local retention was reduced relative

to fall (4 % vs. 18 %). This led to an increased loss of particles to DS (59 % vs. 40 %). Settlement in the GSC increased for NEP-spawned particles (23 % vs.
unit15%), but decreased for those spawned in the SF (24 % vs. 47 %). Loss of SF-spawned particles to DS also increased (49 % vs. 12 %). These differences can be explained in terms of seasonal changes in the strength of the around-bank gyre (*Naimie et al.*, 1994, 2001). This recirculatory flow was weak early in the spring, causing particles from the GSC and SF to experience low retention and high losses. Strengthening of the gyre with increased stratification later in the spring caused particles from the NEP to have higher retention. The reverse effect occurred in fall (i.e. the gyre was strong early in the season but weak later) causing higher retention of GSC- and SF-spawned particles and lower retention of NEP-spawned particles.

Altering the depth distribution from *passive* to *pycnocline-seeking* in the spring had a pronounced effect on dispersal and the associated connection fractions (figure 3.5d-f vs. figure 3.5a-c, table 3.1). In spring, *pycnocline-seeking* behaviour increased local retention of GSC-spawned particles as compared to the *passive* case (18 % vs. 4 %, table 3.1) and decreased settlement of NEP-spawned particles in the GSC (0 % vs. 23 %). This is in stark contrast to fall, when depth distribution had negligible effects on these connection fractions. Additionally, *pycnocline-seeking* particles from the NEP settled more frequently in UH (81 % vs. 63 %). Particles from SF also experienced a lower rate of settlement in the GSC (7 % vs. 24 %), and instead settled in UH (51 % vs. 23 %). These changes can be explained by the fact that on-bank retention during spring requires plankton be deep in the water-column (*Werner et al.*, 1993; *Lynch et al.*, 1998; *Gentleman*, 2000; *Lough and Manning*, 2001).

Settlement distributions for *pycnocline-seeking* particles in the spring were similar to those having the same behaviour in fall (figure 3.5d-f vs. figure 3.4d-f). However, this similarity was not borne out in the connection fractions due to inter-seasonal differences in

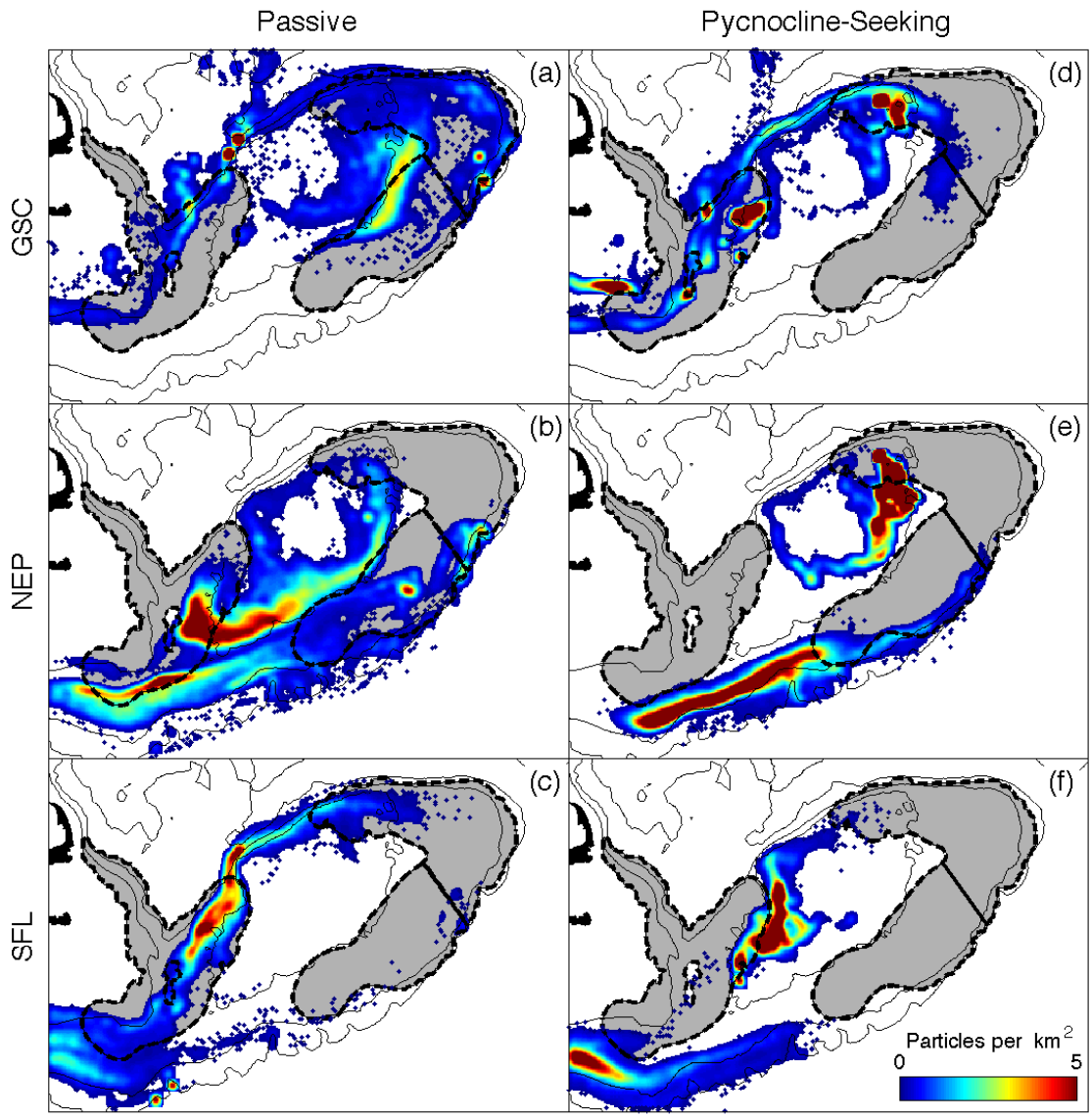

Figure 3.5: Particle distribution in spring for both the *passive* and *pycnocline-seeking* behaviours. The distributions for the GSC-spawned (a and d), NEP-spawned (b and e), and SF-spawned (c and f) particles are each shown separately.

environmental conditions. Loss of GSC-spawned *pycnocline-seeking* particles to DS was greater in the spring than in the fall (51 % vs. 35 %). The portion of NEP-spawned particles settling in the GSC decreased i spring (0 % vs. 13 %), whereas both local retention and settlement in UH increased (14 % vs. 7 % and 81 % vs. 63 %). Similarly, SF-spawned particles were less likely to settle in GSC (7 % vs. 25 %), but more likely to be transported DS or settle in UH (and 41 % vs. 31 % and 51 % vs. 43 %). These differences arose due

the aggregation of larvae at the shallow pycnocline, which caused them to be transported off GB by the strong along-shelf flow.

3.2 Discussion

3.2.1 Larval Depth Distribution & Dispersal

The simulated dispersal of *passive* larvae in the fall is consistent with previous model studies (*Tremblay et al.*, 1994; *Tian et al.*, 2009a), showing that GSC-spawned larvae can be locally retained or settle in both the NEP and SF, whereas local retention of NEP and SF subpopulations is negligible and larvae from both regions settle in the GSC (figure 3.6). This indicates that the simplifying assumptions made here about ascent, descent and Lagrangian residual advection were reasonable and further, these simulations have highlighted some previously unrecognized features of the metapopulation dynamics. For example, while the GSC is the most locally retentive in fall, overall rates of particle retention within the metapopulation in fall are roughly equal for each of the three subpopulations. Additionally, there are noteworthy differences among the subpopulations with regard to which can supply larvae to DS populations, as well as the relative proportion predicted to settle in UH (figure 3.6, table 3.1). Thus, these results demonstrate that the sources, retention and losses are unique for each subpopulation, but their tight coupling through advective exchange of larvae indicates that the function of each subpopulation needs to be considered to study the dynamics of the metapopulation of *P. magellanicus* on GB.

Previous studies were able to identify certain simulated behaviours as unrealistic because they resulted in horizontal distributions that were inconsistent with observations (e.g. *Tremblay et al.*, 1994). By the same approach, the simulations shown here suggest

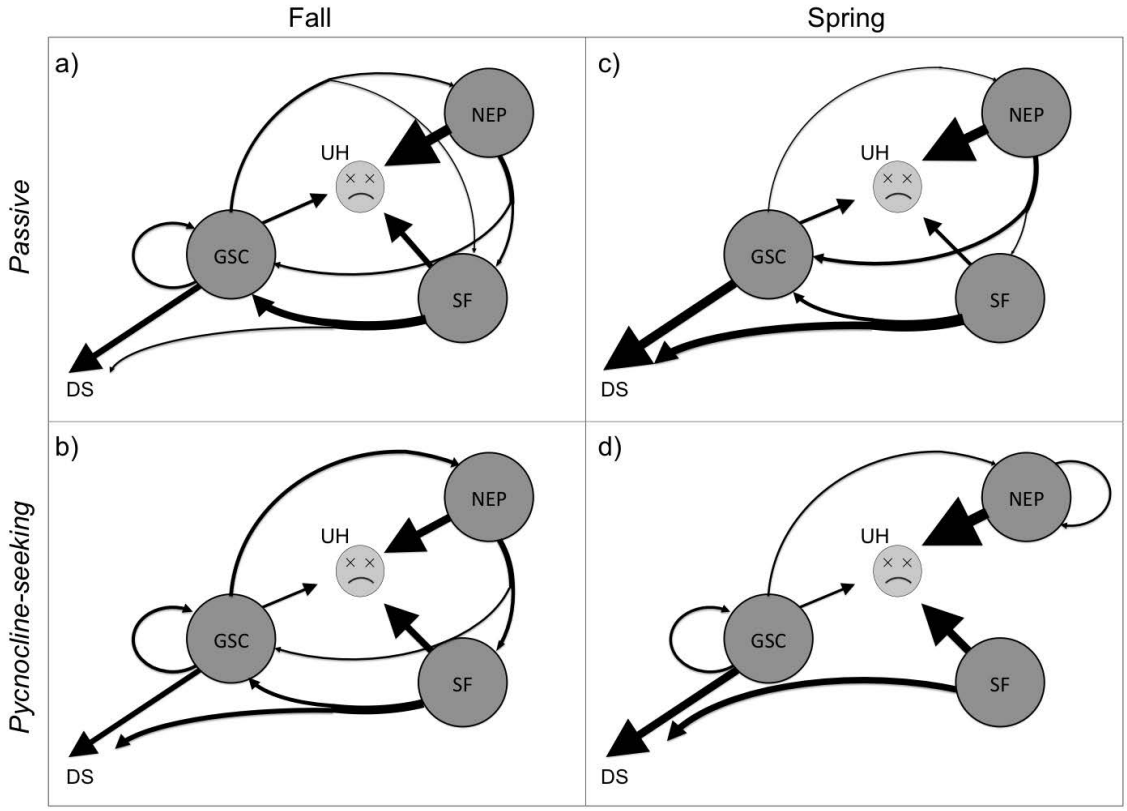

Figure 3.6: Schematic diagrams of model-estimated connectivity for the (a) fall, *passive*; (b) fall, *pycnocline-seeking*; (c) spring, *passive*; and (d) spring, *pycnocline-seeking* cases. Each arrow illustrates the transport of particles among the geographic regions (GSC, NEP, SF, DS and UH), with the thickness of the arrow proportional to the corresponding connection fraction. Small connection fractions (< 8 %) have been omitted from the graphs.

passive behaviour results in unrealistic vertical distributions (figure 3.2), and that model estimates of larval dispersal based on *passive* behaviour may be biased. The novel simulation of *pycnocline-seeking* particles seen here was designed to reflect observed larval depth distributions. In contrast to the *passive* simulation, *pycnocline-seeking* behaviour aggregated GSC-spawned particles on the NEP, where high densities of late-stage larvae and adult scallops are observed (figure 3.1e; *Tremblay and Sinclair*, 1992; *Hart and Chute*, 2004). Hence, *pycnocline-seeking* behaviour seemed to improve modelled distributions on the NEP, but whether this is the case for other regions is difficult to determine without more data for horizontal distributions of late-stage larvae.

The effect of larval depth distribution on predicted settlement was different for each

subpopulation, such that there is a complex relationship between depth distribution and GB metapopulation dynamics. Changing from *passive* to *pycnocline-seeking* behaviour increased the frequency of particle transport from the GSC to NEP, had little effect on NEP-spawned particles, and caused SF-spawned particles to be advected DS instead of being retained in the GSC (figure 3.1, figure 3.6, table 3.1). The effects of behaviour corresponded to changes in the associated connection fractions by factors of 2-5 (table 3.1), which is comparable to the estimated effects of variability in the circulation (*Tian et al.*, 2009a). This is far greater an effect of depth distribution than suggested by previous estimates based on other simplified behaviours (e.g. fixed-depths, surface-seeking, etc.; *Tremblay et al.*, 1994; *Tian et al.*, 2009a).

The influence of larval swimming behaviour may be different than the above results indicate, as larval behaviours are more complex than characterized in this model. The *pycnocline-seeking* behaviour is idealized. For example, it neglects any high-frequency interactions of the physics and biology, which can be chaotic (*Tian et al.*, 2009c). As well, laboratory studies show that larger veliger larvae may swim below the pycnocline (*Gallager et al.*, 1996), which could have significant effects on the retention of NEP- and SF-spawned larvae, as the strength of the around-bank gyre increases with depth. Furthermore, aggregation at the pycnocline has not been linked to any particular behavioural mechanism, and it is possible that larvae are responding to changes in environmental variables that are correlated with the pycnocline (e.g. temperature, food etc.), as opposed to responding to density *per se*. As well, *P. magellanicus* may be selected to vertically migrate such that the risk of predation is decreased, or such that the probability of retention within the GB gyre is increased (*Manuel et al.*, 1996). This suggests the need for more lab, field and model studies focused on understanding how the observed depth distribution emerges from the complex interactions of larvae with their environment.

3.2.2 Larval Growth Rate & PLD

Previous model studies assumed that PLD was the same for all scallop larvae on GB, and that the mean PLD in the fall was ∼35 days based on mean temperatures (*Tremblay et al.*, 1994; *Tian et al.*, 2009a). To investigate the effect of individual thermal history, a model for temperature-dependent PLD was developed, using a Q_{10} relationship. This simple model estimates that the 4 °C cooler mean temperature in spring extends the mean PLD by about 2 weeks. Intra-seasonal spatial variations in temperatures (figure 2.2) led to individual PLDs ranging by more than 10 days (figure 3.3). Changing between *passive* vs. *pycnocline-seeking* behaviours led to statistically significant variations in mean PLD of 1-2 days (figure 3.3), with *passive* being systematically longer, due to particles below the thermocline experiencing colder temperatures. PLD temperature-dependence needs to be considered when larvae experience different temperatures over prolonged periods of time (e.g. variations between years, seasons, regions and/or depths).

Simulations with PLD based on thermal history had similar settlement distributions and connection fractions to those for which PLD was set at a constant mean value (figure 3.3, table 3.1), which supports previous studies of larval transport in fall where this assumptions was made (*Tremblay et al.*, 1994; *Tian et al.*, 2009a). The one notable exception was for SF-spawned *pycnocline-seeking* particles, which showed a dramatic reduction in DS losses due to the influence of the warm slope water. Supply of GB larvae to scallop populations along the New England Shelf and Mid-Atlantic Bight may therefore be sensitive to processes causing pronounced temperature variations on the SF (e.g. intrusion of warm-core rings).

While results show that variation in mean PLD of 1-2 days had little effect, change in mean PLD of a few days does affect retention and exchange among the subpopulations in both seasons. A difference of 5 days in the seasonal mean PLD changes predicted connection fractions by factors of 2-10 for certain subpopulations (figure 3.7). This difference in mean PLD is well within confidence intervals, as variation in settlement size leads to a

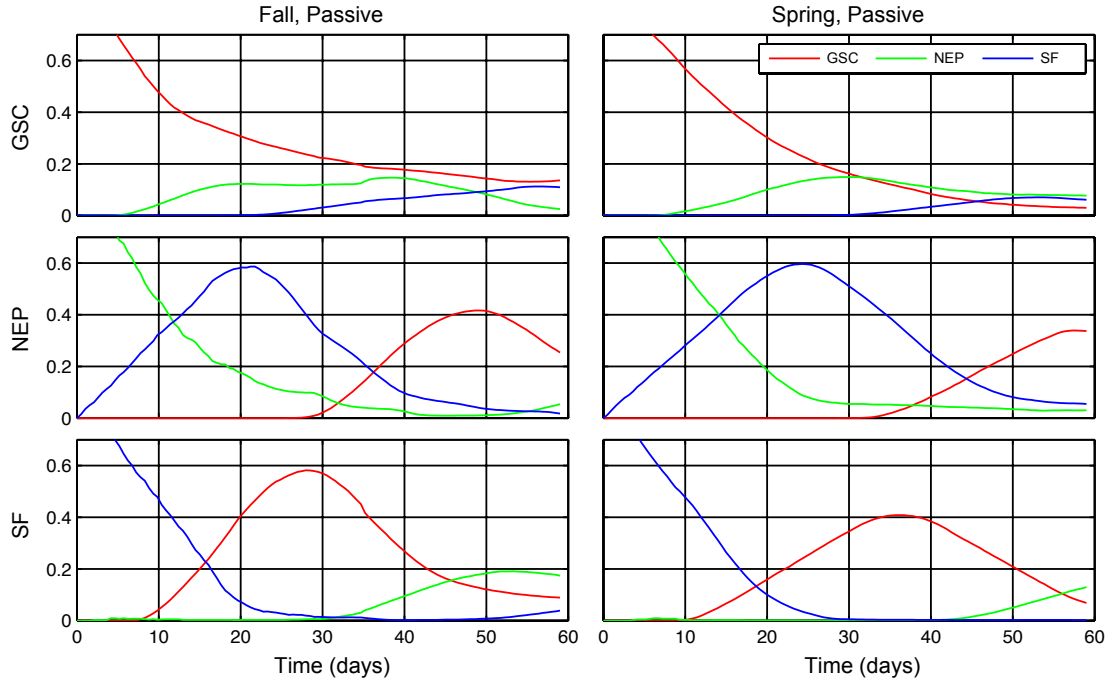

Figure 3.7: Connection-fractions plotted as a function of PLD for the *passive* simulation in fall (left column) and spring (right column). Connection fraction from the source (labeled on the y-axis) to GSC is labeled with circles, while the connection fraction from source to NEP is marked with triangles and source to SF is marked with squares.

range in PLD of 10 days in the fall (*Tremblay et al.*, 1994) and changing Q_{10} from 2 to 2.5 extends the estimated mean spring PLD by 5 days. Furthermore, larvae may extend their PLD if the local benthic habitat is not a suitable substrate (*Culliney*, 1974; *Tremblay et al.*, 1994), and such behaviour has been shown to significantly affect larval transport for other species (*Savina et al.*, 2010). This extended search phase would have a significant effect on dispersal and post-settlement survival of *P. magellanicus* larvae, given that these results – which did not simulate such behaviour – predict large losses of larvae due to settlement in UH (figure 3.6 and 14-81 $\%$, table 3.1). The potential for changes in the mean PLD or an extended search phase to significantly affect larval dispersal indicates the need to improve understanding of these factors.

3.2.3 Spawning Season

It was found that overall retention within the GB metapopulation was lower in spring than in fall. As previously hypothesized, this was due to reduced recirculation of larvae in the around-bank gyre prior to the onset of stratification. The associated losses of SF- and GSC-spawned particles to DS suggest that larvae from these two subpopulations are prime candidates for supplying scallop populations along the New-England Shelf and Mid-Atlantic Bight. However, retention of NEP-spawned particles was higher in spring than in fall, due to intensification of the around-bank gyre in late spring, as compared to the erosion of the gyre in late fall. This suggests high sensitivity of larval connectivity to climate-related changes in stratification.

It is clear from the results that depth distribution influences dispersal of *P. magellanicus* larvae on GB, as has been shown for other planktonic species in the region (*Werner et al.*, 1993; *Lough and Manning*, 2001). Changing between *passive* and *pycnocline-seeking* behaviour in simulations had a larger impact on dispersal and transport connectivity in spring than in fall (figure 3.7, table 3.1). The *pycnocline-seeking* behaviour was based on observations made in the fall, but hydrographic conditions in spring are different from those in the fall (figure 2.2), such that the associated larval behaviours may also be different. Confident prediction of larval retention and exchange in spring is currently limited by lack of observations of the depth-distribution of larvae in spring.

In addition to transport-related connectivity, the number of larvae ultimately recruiting to the metapopulation will depend on survivorship in each spawning season. Survivorship in the spring would be reduced relative to that in fall due to the increased PLD, if mortality rates were the same between seasons. However, spring mortality rates are likely lower in than in fall, because larval mortality rates are typically reduced for lower temperatures (*Houde*, 1989). For example, if the Q_{10} for mortality is the same as that assumed for PLD, then these effects would cancel out and survivorship in both seasons would be

comparable. This warrants more study, along with other factors influencing recruitment, including fecundity and post-settlement survival. In order to understand the metapopulation dynamics for *P. magellanicus* on GB, these additional processes must be examined.

CHAPTER 4

DEMOGRAPHIC FACTORS INFLUENCING LARVAL DISPERSAL

In this chapter, larval dispersal is simulated in order to quantify the influence of two demographic factors on the rates of exchange of *P. magellanicus* larvae among the three major subpopulations on GB. Specifically, the effects of (1) spatial distribution of adults, and (2) seasonal difference in fecundity and mortality are modelled. Additionally, larval dispersal is simulated for two distinct eras in the fishery, allowing the effects that real changes in the demographics associated with anthropogenic factors such as fishing have had on larval connectivity in the GB metapopulation. In order to perform these simulations, fishery data had to be analysed. These analyses were novel, so they shown as results in this chapter (subsection 4.1.1). The simulation results are used to gain insight into the questions raised in chapter 1 and help to guide future research by quantifying the relative impacts that these factors have on larval connectivity.

4.1 Results

4.1.1 Larval Production Fields

The larval production field, $l(x, y)$, was estimated for the *pre-closures* and *post-closures* fishery eras in both the spring and fall for each of the three subpopulations by following the methods described in section 2.3 (figure 4.1). The larval production field describes the density of larvae spawned in each season as a function of space. The total number of scallop larvae spawned in each bed for each season and fishery era is shown in table 4.1. In the *pre-closures* era, the NEP spawned ten times more scallop larvae than the GSC or SF, as estimated by the larval production fields. The NEP spawned 1.3 times as many larvae in the *post-closures* era as in the *pre-closures* era, and the GSC and SF spawned $\sim$5 times as many larvae in the *post-closures* era as in the *pre-closures* era (4.8 times in spring and 5.2 times in fall). As the US fishery recovered, the combined contributions of the GSC and SF increased from 15 $\%$ of total larval production on GB to more than 40 $\%$. The spring accounted for 1/3 of total spawning output within a year and the fall accounted for the other 2/3 (compare row 1 with row 2 in table 4.1).

The increases in larval production experienced in all three subpopulations during the *post-closures* era were due in part to an increase in scallop abundance, and in part to an increase in the mean size of the scallops, which correlates with fecundity. The estimated number of scallops increased from 1.9 M scallops in the *pre-closures* era to 5.7 M in the *post-closures* era. Scallops also became larger in the *post-closures* era, leading to an

$\times 10^{13}$	*pre-closures*			*post-closures*		
	GSC	NEP	SF	GSC	NEP	SF
Spring	71	752	76	340	982	374
Fall	129	1418	143	692	1952	734

Table 4.1: The number of larvae spawned in each bed for each season in each era.

increase in mean fecundity. The factor of five increase in the larval production field in the GSC is explained by a threefold increase in adult scallop abundance, times a factor of 5/3 increase associated with the higher fecundity of the larger scallops. The number of scallops in the SF increased from 1.9 M in the *pre-closures* era to 7.8 M in the *post-closures* era. Thus, the factor of five increase in larval production in the SF was explained by a factor of 4 increase in abundance and a factor of 5/4 increase associated with higher mean fecundity in the scallops. The number of scallops on the NEP was effectively unchanged by the US area closures (18 M in the *pre-closures* era to 19 M in the *post-closures* era). The factor of 1.3 increase in larval production on the NEP was therefore explained almost entirely in terms of increased mean fecundity of scallops.

The larval production fields for each fishery era in each season are shown in figure 4.1. In each of these fields, the distribution of larval production in the GSC can be split up into four distinct regions. These are the northwest section near Cape Cod (N-GSC), the western GSC (W-GSC), the southern GSC (S-GSC), and the largest one in the eastern part of the GSC (E-GSC). These are present in the *pre-closures* era (figure 4.1a,c), but are seen most clearly in the *post-closures* era (figure 4.1b,d). Spawning in the NEP is concentrated near the 80 m and 100 m isobaths, with relatively fewer larvae being spawned near the crest of GB, at the 60 m isobath. In the *pre-closures* era, the US side of the NEP (located by the northern flank and just on the US side of the ICJ line US-NEP) spawned relatively few larvae, whereas the concentration become very high in the *post-closures* era. The larval production field in the SF was highest in the northeastern part of the subpopulation (NE-SF), with relatively fewer larvae being spawned in the southwestern part (SW-SF).

The larval production in spring, relative to total larval production was computed as $100 \times l_{spring}(x,y)/(l_{spring}(x,y) + l_{fall}(x,y))$ (figure 4.2a). The relative contribution of spring spawning varied between 32 $\%$ to 37 $\%$. The relative importance of spring spawning was generally lowest inside the closed areas; scallops tended to be largest in these areas and

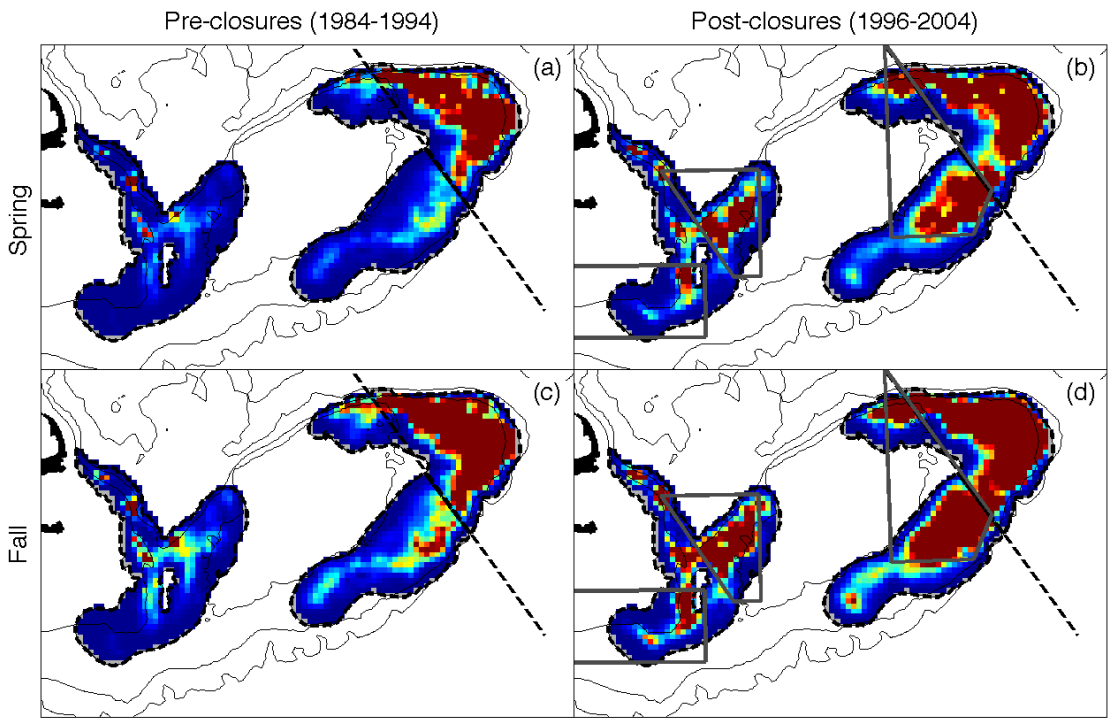

Figure 4.1: The heterogeneous larval production fields in both the *pre-closures* and *post-closures* eras for both the spring and fall seasons. (a) Spring larval production field in the *pre-closures* era, (b) spring larval production field in the *post-closures* era, (c) fall larval production field in the *pre-closures* era, and (d) fall larval production field in the *post-closures* era.

large scallops have relatively higher fecundity in fall than in spring. Regions where spring spawning is relatively more important (i.e. orange regions) indicate a smaller mean size of adult scallops. The scale of this variability, however, is clearly insignificant relative to inter-seasonal variation in fecundity and larval transport. Spatial variability in size-structure is therefore negligible in determining the difference between spring and fall larval production fields. The spring field can be well approximated as one half the corresponding fall field.

The larval production field changed systematically across eras, with the number of larvae produced in the N-GSC, S-GSC and E-GSC increasing by more than a factor of 10, while the rest of the GSC was relatively unchanged (figure 4.2b). The S-GSC corresponds geographically to the NLCA, suggesting that the increase was caused by this closed area. Similarly, the increase in spawning capacity of the E-GSC was caused by CA I. The increase in larval production in the N-GSC did not occur in a closed area. The mean shell

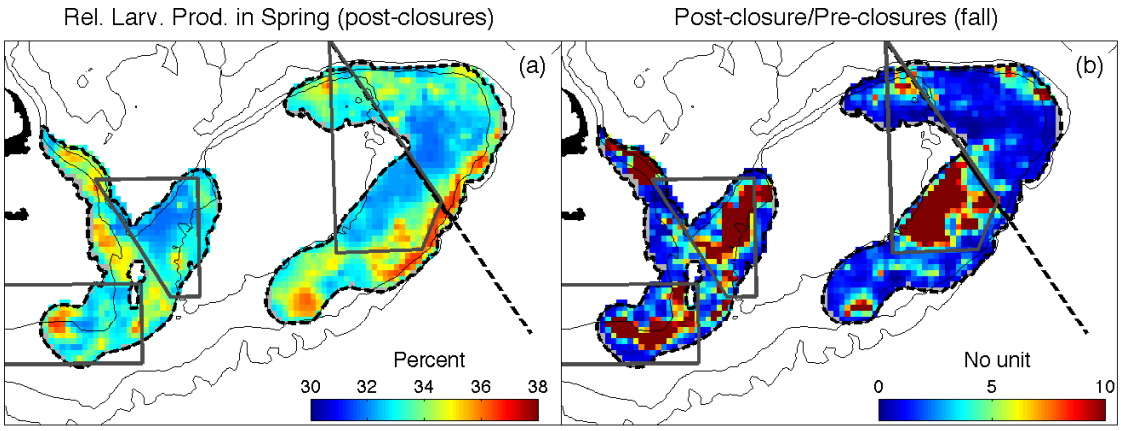

Figure 4.2: Comparison of larval production fields (a) across season and (b) across fishery era. (a) The percentage of larvae spawned in spring, $100 \times l_{spring}(x,y)/(l_{spring}(x,y) + l_{fall}(x,y))$. Relatively low spring contributions (light blue) correspond to regions where the mean size of scallops is higher and high spring percentage corresponds to regions where mean scallop size is small. However, this ratio only varies by a few percentage points. (b) The ratio of the *post-closures* era larval production field the *pre-closures* era larval production field in fall. The red areas indicate drastic increases ($>$ 10-fold) in the number of larvae produced due to the area closures. The increases correspond to the placement of the closed areas, with the NE-SF and US-NEP caused by CA II, that in E-GSC by CA I and that in S-GSC by NLCA. The increase in the N-GSC does not occur inside a closed area.

height of adult scallops in this region did not increase. The increase in larval production was therefore driven by increased scallop abundance. This differs from the increases in larval production that occurred in closed areas, as those were driven in part by increases in mean size of adult scallops. Larval production in the SF increased mostly within the NE-SF, while that in the rest of the subpopulation was relatively unchanged. This region coincides with the southern extend of CA II. The NEP changed very little, with the exception of the US-NEP, where larval production was increased by factors of 3-10.

4.1.2 Effect of Heterogeneous Scallop Distribution on Larval Dispersal

To evaluate the impact of a *heterogeneous* scallop distribution on larval connectivity, two simulations were run and compared. In the first simulation, all super-individuals spawned within each subpopulation were taken to represent the same number of larvae. This number was determined by dividing the total number of larvae spawned by the number of super-individuals seeded in each subpopulation. This initial distribution of larvae is

referred to here as the *homogeneous* larval production field. The second simulation used the *heterogeneous* larval production field shown in figure 4.1d, where the number of larvae represented by each super-individual is determined by the local value of the larval production field, $l(x_{ind}, y_{ind})$ (see section 2.3). The *homogeneous* and *heterogeneous* larval production fields both represent the same total number of larvae, and differ only in the spatial distribution of the larvae at the time of spawning. The analysis below was performed for both fishery eras and for both behavioural assumptions in the particle-tracking model, with temperature-dependent PLD and constant mortality rate. However, only the *post-closures* era simulation with *pycnocline-seeking* behaviour is shown here.

The simulation with a *homogeneous* larval production field, *pycnocline-seeking* behaviour and *constant* mortality was run in fall to establish a baseline against which to compare the effects of *heterogeneous* scallop distribution. The result reflects the particle distributions of chapter 3, except with the larval distribution in each frame scaled by a factor proportional to the number of larvae spawned in that bed (figure 4.3a-c). Thus, the plots show the simulated settlement distribution of a number of larvae instead of a distribution of "particles". The new simulation highlights the difference in the number of larvae spawned in each bed, with 3 times more NEP-spawned larvae than GSC or SF-spawned larvae present at the time of settlement. The entries in table 4.2 quantify this effect, with the column corresponding to NEP increasing relative to the GSC and SF. In contrast to the particle connectivity matrix in chapter 3 where all three subpopulations appeared to be equally important to the metapopulation, the larval connectivity matrix shown here suggests that the NEP is the largest contributor of larvae to each of the three subpopulations.

Next, the simulation was re-run, but with the *heterogeneous* larval production field. The distribution of super-individuals was identical in each simulation because the same physics and larval behaviour were simulated in both cases; only the number of larvae represented per ensemble particle was different. In order to highlight the change in connectivity that

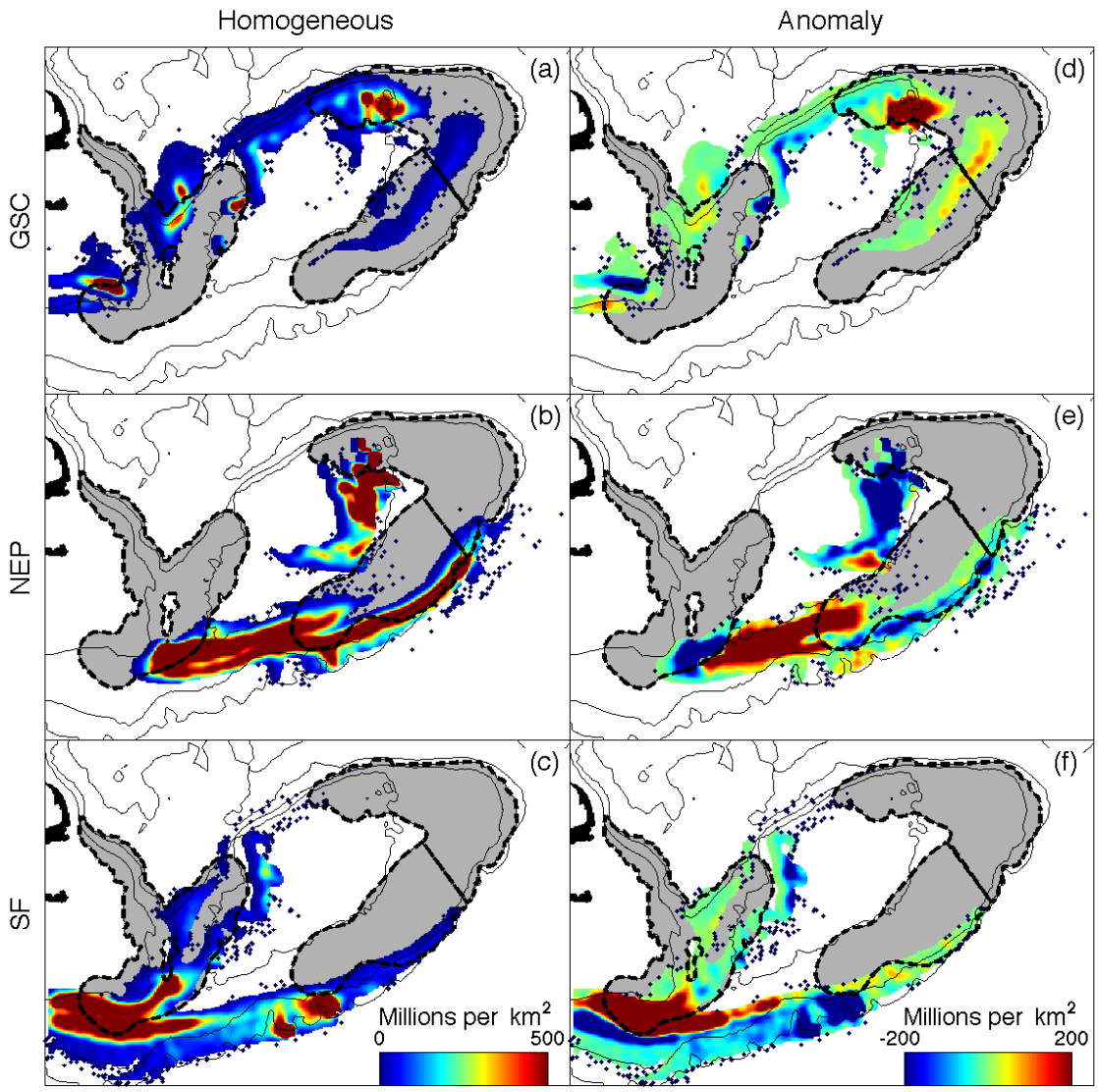

Figure 4.3: Larval settlement distributions in fall for different larval production fields. The *homogeneous* simulation is shown in frames (a-c); and and the change in larval distribution due to the *heterogeneous* larval production field is shown in frames d-f.

		Homogeneous			Heterogeneous		
	Settlement	Spawning			Spawning		
Description	Region	GSC	NEP	SF	GSC	NEP	SF
Number Settling (10^{10})							
	GSC	40	111	97	28	64	179
	NEP	47	52	0	76	22	0
	SF	3	121	3	5	126	4
	UH	37	407	265	22	406	202

Table 4.2: Larval connectivity for *homogeneous* and *heterogeneous* larval prouction fields. The simulation used *pycnocline-seeking* particles in fall environmental conditions, with a *constant* mortality rate.

considering a *heterogeneous* larval production field had on larval connectivity, a plot of the anomaly (*heterogeneous* − *homogeneous*) in larval settlement distribution was made (figure 4.3d-f). Changing from the *homogeneous* to the *heterogeneous* larval production field in the GSC led to an increase in the number of larvae arriving in the the NEP (as indicated by the dark red region in the norther part of the NEP in figure 4.3d). The high density aggregation of larvae spawned in the eastern edge of the GSC (GSC-E) in the *heterogeneous* adult distribution caused this difference. This led to an increase in the number of GSC-spawned larvae arriving at the NEP from 470 billion to 760 billion – a 60 % change (table 4.2). Local retention of larvae within the GSC decreased from 400 billion to 280 billion – a 30 % decrease. The number of larvae settling in UH was also lower for the simulation with a *heterogeneous* larval production field. These effects were all present, independent of the simulated behaviour or era (*not shown*). In each case, the large number of larvae spawned in the GSC-E were transported to the NEP.

Larvae spawned in the NEP near the 60 m isobath tended to move onto the crest and either settled in UH, or were retained in the NEP. Consequently, changing from *homogeneous* to *heterogeneous* spawning decreased the total number of larvae settling in these regions because the number of larvae spawned near the 60 m isobath were decreased. The blue region in the crest (figure 4.3e) indicates this decrease, which is also reflected in table 4.2 (520 billion larvae settling in NEP vs. 220 billion larvae). The number of larvae reaching the GSC decreased for the same reasons, because fewer larvae were spawned near the NEP-SF border (blue area in figure 4.3e; 1,110 billion larvae vs. 640 billion larvae settling in GSC). These larvae were instead spawned in the middle of the NEP, leading them to ultimately settle in the UH on the flank of GB between the SF and GSC (red spot in figure 4.3e).

The number of SF-spawned larvae settling in the GSC was drastically increased from 970 billion to 1,790 billion larvae (table 4.2). The high concentration of larvae spawned

in the northeastern part of the SF arrived for settlement in the southernmost part of the GSC, while settlement in the rest of the GSC was relatively unchanged (see the red area in figure 4.3f). The same effects were seen when larvae were simulated with *passive* swimming behaviour, except that the increased settlement in the GSC was concentrated in the eastern part that is responsible for seeding the NEP (*not shown*). The number of larvae from the SF arriving at the GSC was even higher, with larval settlement in the GSC increasing from 1,560 billion to 2,700 billion larvae.

4.1.3 Larval Dispersal in Spring

The *heterogeneous post-closures* larval production field for spring was used to simulate larval transport in spring with *pycnocline-seeking* behaviour and individually-varying PLD. Constant larval mortality of 20 $\%$ per day was first simulated (i.. $Q_{10} = 1$). The resulting larval connectivity was much lower than in fall, with no more than 40 billion larvae being retained within any subpopulations (table 4.3). At the time of settlement around 48 days, the total number of simulated larvae was about 2.5 $\%$, or 1/40th the number of settling fall-spawned larvae. The increase in mean PLD led to a reduction in the net survivorship of larvae, because larvae were exposed to a constant mortality rate for a longer period of time. After 36 d (the mean PLD in fall) with mortality of 20 $\%$d^{-1}, approximately 1 in 2,500 larvae survive, whereas 1 in 45,000 larvae survive after a PLD of 48 d (the mean PLD in spring). The lower fecundity in spring accounts for a reduction of one half in the number of settling scallops, while the extended PLD accounts for the remaining factor of 1/20th. The total number of larvae settling within the GB metapopulation was 80 billion (table 4.3), whereas the corresponding fall simulation predicted that 5 trillion larvae would be retained within the metapopulation (table 4.2). The reason that spring-spawned larvae represented only 1.6% as many larvae settling in the metapopulation, as opposed to the 2.5 $\%$ predicted by counting the number of simulated larvae, was that transport in spring leads to lower retention of super-individuals (see figure 3.5d-f). Thus, transport accounted for a factor

Description	Settlement Region	Constant m Spawning GSC	NEP	SF	T-dependent m Spawning GSC	NEP	SF
Number Settling (10^{10})							
1. Spring	GSC	4	0	1	40	0	7
	NEP	1	2	0	32	48	0
	SF	0	0	0	1	9	0
	UH	1	26	8	23	345	78
2. Spring:Fall (%)	GSC	13	0	0	81	0	6
	NEP	2	11	-	25	183	-
	SF	0	0	0	7	4	0
	UH	5	6	4	57	68	62

Table 4.3: Larval exchange rates in spring. (Row 1) The number of simulated larvae (tens of billions) settling in each subpopulation under (left column) constant mortality rate and (right column) temperature-dependent mortality rate. (Row 2) The ratio of larval exchange in spring to that in fall, indicated as a percentage. A '-' indicates that no larvae were exchanged in either season, so the ratio is undefined.

1.5 reduction in larval retention within the metapopulation, lower spring fecundity a factor of 2, and larval mortality a factor of 20. The amount of loss due to transport was smaller for *passive* behaviour (chapter 3), leaving only fecundity and mortality as relevant factors determining the difference between spring and fall connectivity (*not shown*). Migration rates among the subpopulations ranged between 0 and 40 billion, with GSC-spawned larvae settling in the GSC and NEP, NEP-spawned larvae being retained in the NEP, and SF-spawned larvae settling in the GSC.

- Reran with Q10 = 2 (reason for this in methods) - describe the results

Of the three factors considered here, net larval mortality contributes by far the most to reducing simulated larval connectivity in spring. However, the value of this quantity in reality is unknown and may be sensitive to numerous unmodelled factors. Here, the possible effects of these unmodelled factors on mortality rate were linked to temperature as a proxy by changing the simulated Q_{10} factor to 2 (see subsection 2.2.3). This led simulated larval retention in spring to increase from 80 billion to 1.4 trillion larvae – 28% as many as the 5 trillion retained in the fall simulation. Not all *migration rates* (see

glossary) were impacted equally by the change in simulated mortality rate. Though the number of GSC-spawned larvae settling in the GSC increased by a factor of 11, the number of NEP-spawned larvae settling in the NEP increased by a factor of 20. This was due to spatial variation in temperature. Water near the NEP is cooler than that near the GSC, and super-individuals in the NEP experienced temperatures that were 0.6 °C cooler on average. Migration rates were between 0 % to 183 % as large as their corresponding rates in fall, with more NEP-spawned spring larvae settling locally in spring than in fall.

4.1.4 Change in Larval Dispersal Across Fishery Eras

To simulate the change in larval connectivity that has occurred within the GB scallop metapopulation between the years 1984-2004, simulations were run using both the *pre-closures* and *post-closures heterogeneous* larval production fields in fall with *pycnocline-seeking* behaviour and individually-varying PLD and mortality. The concentration of NEP-spawned larvae at the end of the simulated PLD was substantially higher than that for those spawned in other beds (figure 4.4a-c), because more larvae were spawned in the NEP than in the GSC or SF (table 4.1). Of simulated GSC-spawned larvae settling within the metapopulation, the majority settled locally (140 billion; table 4.4), while half as many settled in the NEP. Large numbers of NEP-spawned larvae settled in the SF (940 billion), while many also settled in the GSC, particularly in the S-GSC region. Local retention was low, with only 70 billion NEP-spawned larvae being retained. SF-spawned larvae settling in the GSC (270 billion, in total) were concentrated in the S-GSC region. In total, 2 trillion larvae spawned in the *pre-closures* settled somewhere within the metapopulation, with the majority (1.5 trillion; 75 %) being spawned in the NEP.

The effect of the fishery closed areas on larval connectivity in scallops on GB was evaluated by comparing the simulated larval settlement distributions associated with the *pre-closures* era to those of the *post-closures* era. After the area closures, the number of larvae spawned

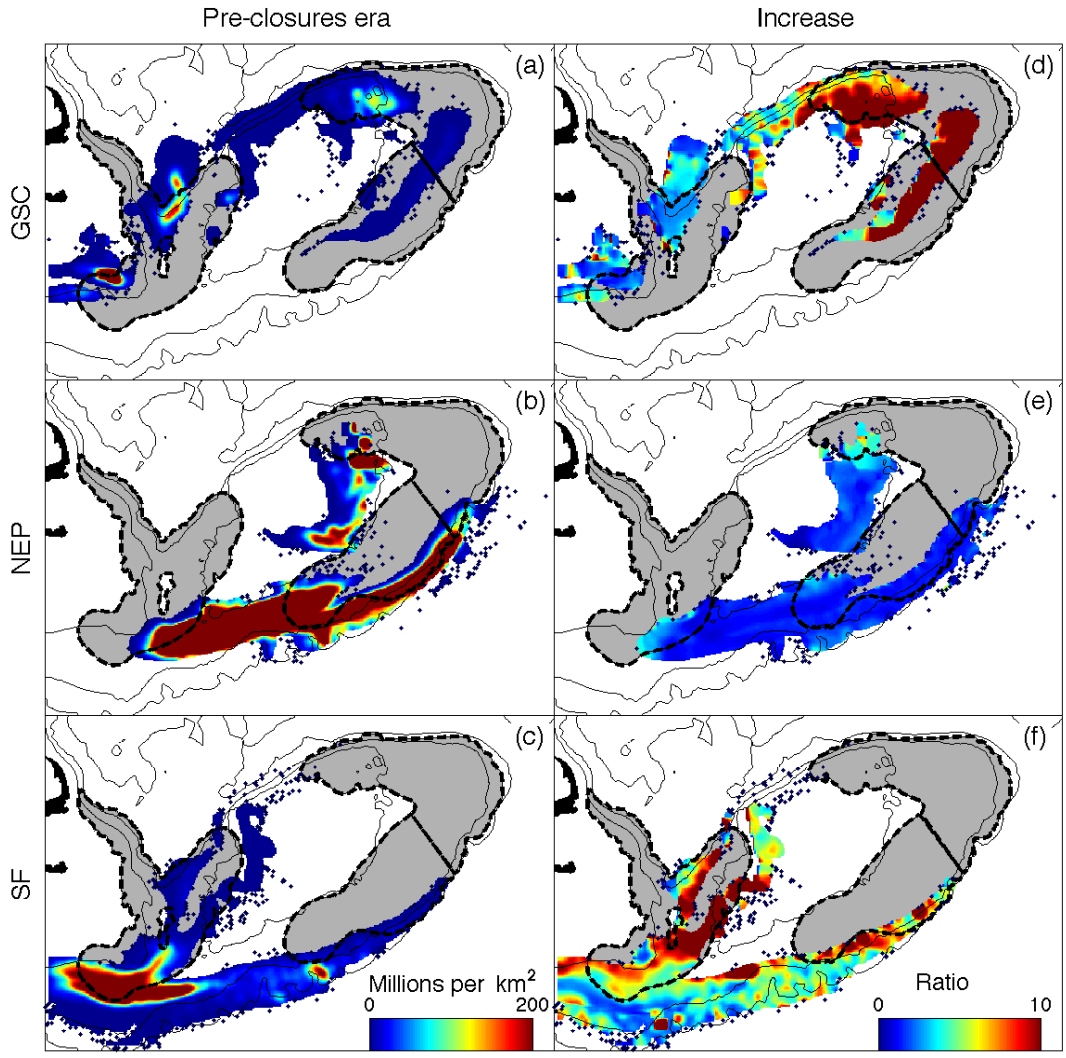

Figure 4.4: Larval settlement distribution in different fishery eras. The *pre-closures* era (a-c), the *post-closures* era (d-f), and the increase in larvae in the *post-closures* era (g-i). The increase is plotted as a ratio – the *post-closures* settlement distribution, divided by the *pre-closures* distribution.

		Pre-closures m			Post-closures/Pre-closures		
	Settlement	Spawning			Spawning		
Description	Region	GSC	NEP	SF	GSC	NEP	SF
Number Settling (10^{10})							
	GSC	14	50	27	2.0	1.3	6.5
	NEP	7	7	0	11.1	3.1	2.0
	SF	0	94	1	16.9	1.3	7.2
	UH	5	301	45	4.2	1.3	4.5

Table 4.4: Larval connectivity in different fishery eras. The number of scallop larvae settling in each subpopulation in the *pre-closures* era (left) and the factor increase in larval settlement that occurred in the *post-closures* era (each computed as ℓ_{post}/ℓ_{pre}).

within the GSC and the SF increased 5-fold (table 4.1). There were two migration rates in particular that increased drastically in the *post-closures* era. First, the number of simulated GSC-spawned larvae settling in the NEP increased 11-fold from 70 billion larvae up to 760 billion larvae (table 4.4 vs. table 4.2). Second, the number of SF-spawned larvae settling in the GSC increased from 270 billion to 1.8 trillion. Both of these increased migration rates were due directly to increases in adult scallop abundance and size in CA I (E-GSC) and CA II (NE-SF). The increase in larval production that occurred in the E-GSC led to an increase in the number of larvae that settled in the NE-SF. The increase in larval production that occurred in the NE-SF also increased the number of larvae that settled in the E-GSC. Thus, the local scallop populations in the NE-SF and E-GSC appear to be coupled. Both of these regions are inside closed areas; thus the closed areas (CA I and CA II) are coupled. The number of larvae settling in the NEP also corresponded to the increase in larval production in the E-GSC. Similarly, an increase in larval settlement in the S-GSC was related to increased larval production in the NE-SF. Local retention of GSC-spawned larvae doubled (from 140 billion to 280 billion; table 4.2 vs. table 4.4), and this was due primarily to the increase in the number of scallops in the N-GSC near Cape Cod. Local retention of NEP-spawned larvae within the NEP experienced an increase, which was associated with the larger numbers of larger scallops in the US-NEP. The total number of larvae that settled in the metapopulation was 5 trillion, reflecting a factor of 2.7 increase in larval supply due to the closed areas. The additional larvae were primarily spawned within closed areas in the US. The dominant role of NEP-spawned larvae that occurred in the *pre-closures* era became less prominent in the *post-closures* era, with 42 $\%$ of successful larvae coming from the NEP, while 22 $\%$ were from the GSC and 36 $\%$ from the SF.

4.2 Discussion

4.2.1 Scallop Distribution & Larval Dispersal

Though previous studies have modelled heterogeneous distribution of scallops on GB (*Tremblay et al.*, 1994; *Tian et al.*, 2009a,b), this is the first investigation into its effect on larval connectivity. Changing from a *homogeneous* to a *heterogeneous* larval production field changed simulated migration rates by up to a factor of 2. Accurate representation of scallop distribution within each subpopulation, though less important than accurately modelling larval swimming behaviour, appears to be important. The ocean currents modelled in this thesis were not resolved below the mesoscale (kilometers to tens of kilometers), so resolving patchiness in scallop distribution at any resolution finer than the mesoscale is unlikely to improve these model simulations further.

In all simulations performed for the study in subsection 4.1.2, regardless of fishery era or depth-distribution, changing from a *homogeneous* to a *heterogeneous* larval production field increased the number of SF-spawned larvae that arrived in the GSC. The change was due to the relatively high abundance of reproductive scallops in the NE-SF. This suggests that it is the state of the spawning stock in the NE-SF, rather than that of the entire SF, that impacts recruitment in the GSC. The same was true for the E-GSC – the number of GSC-spawned larvae settling in the NEP depended on the number spawned in the E-GSC, not the rest of the GSC. The fact that larval exchange is really among smaller regions has potential implications for the design of experiments for determining stock-recruitment relationships (e.g. *Mcgarvey et al.*, 1993). More generally, this result suggests that the complexity of larval exchange within the GB metapopulation is not captured by the three large subpopulations that were defined for this and previous particle-tracking studies (e.g. *Tremblay et al.*, 1994; *Gilbert et al.*, 2010). Subpopulations should be defined based not only on the spatial distribution of adults as was done in this thesis, but based also on the

surrounding oceanography and potential transport pathways.

The N-GSC scallop aggregation near Cape Cod was responsible for a large portion of the total larval production within the GSC. Larvae spawned in this area settled in the GSC and appear to be candidates for seeding the S-GSC and E-GSC in particular (figure 4.3), which would situate their progeny for likely retention within the GB metapopulation. However, the N-GSC aggregation of scallops did not receive larvae in any simulations. This is consistent with general knowledge of the circulation in the area, where currents tend to be alongshore to the south/southeast (*Limeburner and Beardsley*, 1982), and thus would not transport larvae in the opposite direction. This raises the question of where these scallops come from, since they are potentially important contributors to the GB metapopulation dynamics. To the best of the author's knowledge, the potential for scallop larvae spawned in the Gulf of Maine to reach the N-GSC has not been examined, but the direction of the currents in the region suggest it as a possibility worth investigating through particle-tracking, or *in situ* investigation.

The NEP spawns more larvae than the GSC and SF (table 4.1). Yet, a large number of these larvae settled in the unsuitable habitat located between the SF and GSC (figure 4.3b,e). This effect was increased in simulations with *heterogeneous* larval production fields. Though the simulations consistently suggest that these larvae settle in UH, a longer PLD would move these larvae into the GSC. As suggested in chapter 3, if pediveliger larvae were to extend their PLD for several days or weeks, then they could gain the potential to reach this suitable habitat and maintain themselves within the metapopulation. Thus, the simulations shown here emphasize the importance of further study on this aspect of the scallop life-history.

4.2.2 Seasonal Differences in Fecundity & Mortality

Larval survivorship in the spring and fall are both unknown and may vary over orders of magnitude. By comparing two simplified assumptions about larval mortality rates, it

was shown that the range of uncertainty in this parameter has a much larger effect on larval exchange in spring than other factors such as fecundity and transport. Assuming that daily mortality rates in spring were the same as those in fall (i.e. $Q_{10} = 1$) predicted an insignificant contribution of spring-spawned larvae to population connectivity. However, a slight reduction in spring mortality rate ($Q_{10} = 2$) increased survivorship in spring, such that spring-spawned larvae accounted for 20 $\%$ of larvae at settlement. There is no reason to believe that larval mortality rates in spring are the same as those in fall. Biotic and abiotic factors that typically influence mortality in meroplankton vary between the spring and fall seasons on GB. For example, zooplankton (*Davis*, 1987), phytoplankton (*O'Reilly and Zetlin*, 1998) and hydrography (*Ashjian et al.*, 2001) are all different between the two seasons. Furthermore, seasonal effects on settlement and post-settlement success of scallops are possible. A realistic estimate of net larval survivorship in spring is the most important step to understanding the role of spring spawning in the GB scallop metapopulation.

The relative contributions of spring and fall spawning to larval production is a function of scallop size (table 2.1). Thus, spatial variation in the relative contribution of spring-spawning to total larval production is directly related to spatial variation in size-structure of adult scallops on GB. However, the spatial variability in the relative contribution of spring spawning to larval production was small, such that larval production fields in spring are accurately approximated as 33 $\%$ of total annual larval production (figure 4.2a). This suggests that the size-structure of scallops on GB does not have an important effect on the relative impact of spring vs. fall spawning to larval connectivity.

4.2.3 Change in Larval Connectivity Across Eras

The NEP represented 80 $\%$ of total estimated larval production in the *pre-closures* era, which is compatible with other estimates of scallop abundance in the NEP (84 $\%$; *Mcgarvey*

et al., 1993). In simulations, the majority of NEP-spawned larvae settled in unsuitable habitat. Despite this low retention rate, the NEP accounted for the majority of larval settlement within the metapopulation. This was because the number spawned in the NEP was much higher than in the other subpopulations (table 4.1). The settlement distribution of NEP-spawned larvae was unchanged in the *post-closures* era. However, the number of GSC-spawned larvae settling in the NEP, and the number of SF-spawned larvae settling in the GSC increased drastically after the area closures. Both of these changes occurred inside of CA I and CA II respectively, which strongly suggests that these were the causes of the increase. In the *post-closures* era, the central role of the NEP was less pronounced. Real changes to the states of the subpopulations that occurred over time thus had a profound influence on larval connectivity on GB.

The increase in larval production in the GSC and SF were due to the area closures. Estimated scallop abundance and distribution within the closed areas increased by factors of 3-4, while mean size also increased. This is compatible with the 18-fold increase in biomass reported by *Hart and Rago* (2006) for the same years, since that increase was due to the combined effect of increasing scallop abundance and meat weight. There were also increases in the *post-closures* era that did not occur in any closed area. These occurred in the NEP, the SW-SF and N-GSC. The increases in the NEP and SW-SF may be attributable to increased recruitment due to the area closures, as they both received increased larval supply in simulations due to the area closures. However, this explanation appears to conflict with *Hart and Rago* (2006), who found no significant increase in recruitment due to the area closures. The increased larval production in N-GSC likely cannot be attributed to this effect, because no larvae from the closed areas settled in this region in simulations.

The total number of larvae retained within the metapopulation increased approximately in proportion to the increase in the spawning capacity of the metapopulation. The effects have not been evenly distributed, however, with migration rates increasing for some

subpopulations much more than for others (table 4.4). While local retention within the GSC and NEP doubled in simulations, the about of GSC-spawned larvae settling in the NEP increased 11-fold, and the number of SF-spawned larvae settling in the GSC increased 6-fold. These drastic increases in larval exchange are associated with the largest increases in scallop density, which occurred in the E-GSC and NE-SF. It is these two regions in particular that appear to retain the largest number of larvae within the metapopulation. Recruitment of new scallops, and thus population connectivity (see appendix B), did not increase significantly in the *post-closures* era, despite this probable increase in larval connectivity. This lends support to the theory that density-dependent effects, as opposed to limited larval supply, inhibit further growth in the US side of the fishery (*Hart and Rago*, 2006).

CHAPTER 5

CONCLUSION

Effective management of *P. magellanicus* for any particular subregion of GB requires a process-oriented understanding of the effect of climate on the connectivity among the GB subpopulations. In chapter 3, it was shown that biological responses to changes in temperature and stratification affect larval transport among GB subpopulations, as well as the extent to which they can supply downstream regions. Specifically, variation in larval depth-distribution, planktonic larval duration, and the previously overlooked issue of spawning seasonality result in changes to retention and exchange that are comparable to the effect of inter-annual variation in the currents. These simulations have also demonstrated that uncertainty associated with these biological factors leads to high uncertainty in predicted larval dispersal.

In chapter 4, it was shown that larval connectivity is sensitive to mesoscale variability in scallop abundance and this suggests the need to consider these scales when discussing population connectivity in GB scallops. The lack of knowledge on net survivorship of larvae in spring was shown to be the most important factor in determining whether spring-spawned larvae contribute significantly to population connectivity and how this contribution may affect the dynamics of the metapopulation. Finally, simulations suggested that the recovery in landings on the US side of GB associated with the fishery closed areas

implies that larval connectivity has increased as a result. This failed to explain a lack of significant increase in recruitment outside of the closed areas, suggesting that recruitment is inhibited by some other mechanism.

5.1 Recommendations for Future Work

This work has emphasized the need for several specific lab, field and modelling studies if the relationship between anthropogenic, climatic, and biophysical factors are to be used to the benefit of the scallop fishery on GB.

Simulations comparing the effect of different vertical swimming behaviours on larval transport produced up to a factor of five change in the simulated connection fractions. The *pycnocline-seeking* behaviour simulated here appears to be more realistic than the *passive* behaviour in the fall, but it was still simplified. The importance of depth-distribution in determining population connectivity suggests the need to understand how the larval depth-distribution emerges from biophysical phenomena, and how it evolves over the PLD. Larval depth-distribution in spring is unknown, so any observations of this distribution in spring would contribute to our ability to diagnose population connectivity.

Simulations of a temperature-sensitive PLD suggested that variation in temperature within a season is relatively unimportant. However, the effect of inter-seasonal variation in temperature on PLD was shown to be significant. It was shown that this is due to differences in the mean PLD, and that proper estimation of the mean PLD of scallop larvae on GB would improve confidence in estimates of population connectivity (e.g. figure 3.7).

The possibility of significant migration of larvae during or shortly after settlement was ignored in this thesis. However, the simulated settlement distributions, especially of NEP-spawned larvae (see chapter 4) suggest that any behaviour which extended the search-phase

of the larvae could drastically decrease the number of larvae which ultimately settle in unsuitable habitat, especially the connectivity from NEP to GSC. This suggests the need to establish whether larvae can extend their planktonic existence if connectivity is to be estimated confidently.

The simulations comparing larval dispersal with *heterogeneous* spawning fields to those with *homogeneous* spawning fields indicate that the mesoscale variability in scallop distribution must be considered in models of scallop population connectivity. This adds further justification to recent efforts to characterize the distribution of scallops in US waters using high resolution video surveys (e.g. *Stokesbury et al.*, 2004).

The potential for spring-spawned larvae to contribute significantly to the metapopulation dynamics on GB was suggested by *DiBacco et al.* (1995) 16 years ago, yet no previous particle-tracking studies have investigated the implications of this spawning for population connectivity until now. These simulations suggest that spring-spawned larvae may easily account for as much as $1/5^{th}$ of the total larval supply to the metapopulation. However, this estimate was based on several assumptions about larval swimming, spawning and most importantly, mortality rates. An understanding of the potential importance of these larvae to the metapopulation and ultimately the success and stability of the fishery, requires that more be learned about these factors.

The focus of this thesis has been on understanding how biological and demographic factors impact larval dispersal and connectivity in scallops on GB. The simulated physical environment was simplified in order to facilitate these investigations. The next logical step in modelling larval dispersal is to apply the lessons learned here to a more realistic spatially and temporally varying hydrodynamics, such as those advocated by **?**. The presence of scallops in the N-GSC suggests that the Gulf of Maine supplies some larvae to GB. Particle-tracking could prove to be a cheap, appropriate method for understanding the link between GB and potential upstream sources, or even how populations of *P. magellanicus*

are connected over the species' entire range.

APPENDIX A

SCALLOP LIFE HISTORY

P. magellanicus is a bivalve mollusc. Each scallop begins life as an egg, which is fertilized externally. Upon fertilization, the egg will hatch into a larva. The larval stage is typically divided into three phases – (1) trochophore, (2) veliger and (3) pediveliger and these phases are roughly correspond with its (1) ascent, (2) residence and then (3) descent within the water column. Newly settled juveniles typically develop for 2 years before achieving reproductive maturity and may live up to an age of $\approx$12 years as adult before succumbing to senescence. Figure A.1 shows a graphical summary of this life-history.

A.1 Spawning and Eggs

Scallops are highly fecund – reproductive females spawn between 1-270 million eggs. The eggs are negatively buoyant and stay near the benthos until fertilized by a sperm. Spawning is typically synchronous and relatively quick, with all eggs being released within a few weeks (*Posgay and Norman*, 1958; *Langton et al.*, 1987), though protracted spawning events lasting up to two months on GB have been observed within some years. The GB population has one major spawning event in fall in September-October, and spring spawn in May-June occurs in at least some years (*DiBacco et al.*, 1995). Though the relative

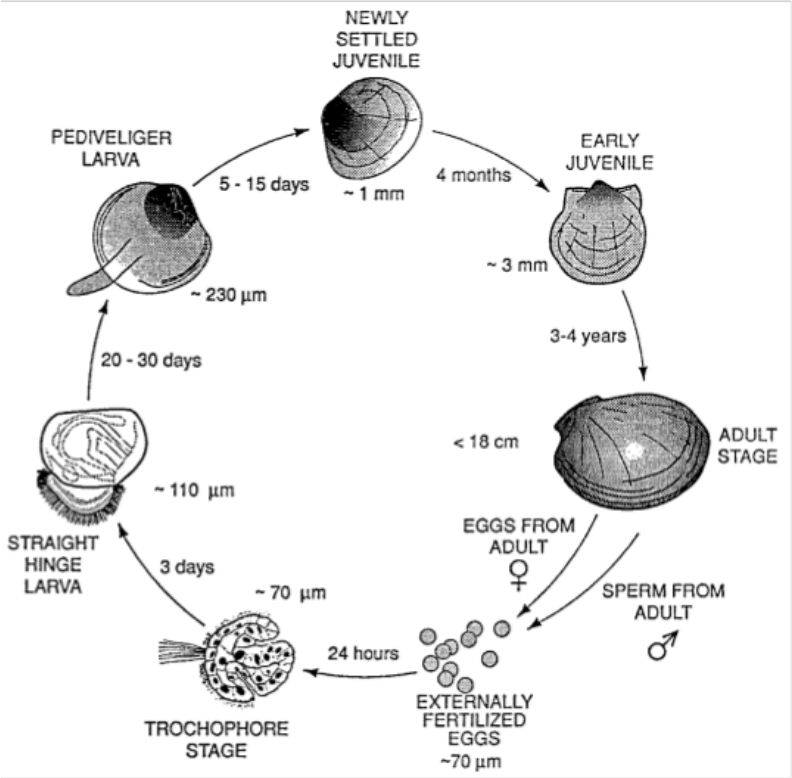

Figure A.1: The sea scallop (*P. magellanicus*) life history. Figure taken from *Hart and Chute* (2004), who got it from *Stewart and Arnold* (1994)

magnitude and consistency of the spring spawn are largely unknown, recent analyses suggest that spring spawning may produce a third to a half as many eggs as in the fall (*DiBacco, pers. comm.*).

A.2 Larvae and Settlement

Upon fertilization, the eggs develop into trochophore larvae and begin their ascent toward the the ocean surface at rates between 0.1-0.7 mms^{-1}. After about 2 days, the veliger phase is reached and the larva stays in the upper water-column, growing to a length of 240-300 µm (*Tremblay et al.*, 1994). The larvae tend to cluster near the pycnocline during this period (*Tremblay and Sinclair*, 1990), though the mechanisms that produce this pattern are not yet well-understood. Mesocosm studies suggest that GB larvae exhibit some diel

migration and that it may be for the purpose of increasing retention (*Manuel et al.*, 1996; *Manuel and O'Dor*, 1997), but migration behaviour has not been observed in the field (*Tremblay and Sinclair*, 1990) and previous model studies suggest that such migration may be beyond the swimming abilities of the larvae (*Tian et al.*, 2009a). Upon reaching the pediveliger phase the larva will descend, prepared for settlement. In a lab experiment, larvae settled more readily in the presence of scallop shells or pebbles than in their absence, suggesting that pediveligers may defer settlement until they can find a suitable settlement substrate (*Culliney*, 1974). Distribution of juvenile scallops in the field also suggest that the pediveligers prefer gravel substrate and may be deferring settlement in hopes of finding this substrate (*Thouzeau et al.*, 1991), though this could also arise simply from differential survival success after settlement.

A.3 Juveniles and Adults

Typically, scallops reach reproductive maturity around age 2. Settled scallops younger than this are considered juveniles. Thus, these scallops are not considered to be successfully recruited to the metapopulation or to the fishery until they reach this age (*Hart and Chute*, 2004). Though spawning may begin at age 2, fecundity is strongly related to age and shell height, such that their fecundity increases throughout their lifetime (*Langton et al.*, 1987). Fecundity likely varies with other factors, such as depth (*Barber et al.*, 1988). Juveniles and adults are not thought to migrate significantly once they join a bed – a tagging experiment suggested that the majority of scallops are displaced by less than 16 km over 2 years (*Posgay*, 1981). The major mechanism of transport of scallops on GB is therefore dispersal in the larval phase.

Phase	Duration	Size	Behaviour
Egg	24 h	4-6µm	Eggs are neutrally buoyant and stay near the benthos until fertilization.
Larva	30-60 d	20-100 µm	Upon fertilization, new (trochophore) larvae rise toward the water surface. They (veligers) then begin to swim and tend to stay near the pycnocline, and have not been observed to migrate vertically in the field. This phase lasts substantially longer than the ascent phase, and possibly the descent phase. Once ready to settle (pediveliger), they sink and may or may not extend their planktonic existence to search for suitable settlement substrate.
Juvenile	2 years	20-100 µm	Juveniles live on the bottom and begin to resemble adults. They do not spawn or spawn negligibly. It is unknown whether (or how) survival is influenced by the season in which the juvenile was originally spawned.
Adult	10 years	20-60 mm	Live on the bottom and are capable of locomotion, but likely do not migrate. Significant spawning begins at age 2 and this magnitude increases throughout the lifetime, up to a maximum of 270 M larvae per spawn.

Table A.1: An outline of sea scallop *P. magellanicus* life-history. The most relevant aspects of the life-history are highlighted, while others are left out.

APPENDIX B

POPULATION CONNECTIVITY

The dynamics of a spatially structured population depend on two separate processes: (1) transport between subpopulations and (2) demographic processes within subpopulations. These two processes are difficult to reconcile simply in one matrix population model, though *Hunter and Caswell* (2005) propose a mathematically sophisticated solution to the problem. A simpler solution has been to focus on only one process at a time; the stage structure of subpopulations can be temporarily ignored by only considering the dichotomy between membership and non-membership in a subpopulation. Entry into a subpopulation is called *recruitment*. The exchange of individuals among subpopulations connects them, and the resulting connectivity among the subpopulations is called the *population connectivity* (*Cowen and Sponaugle*, 2009). Since population connectivity is discussed in this thesis, it is important to be clear which aspects of metapopulation dynamics this concept describes and which it does not. The goal of this appendix is to explain how the matrices described in section 2.4 relate to the concept of population connectivity.

In a spatially structured population (or metapopulation), the number of new recruits arriving to a subpopulation depends (for a benthic marine species such as *P. magellanicus*) on the abundance and fecundity of adults, the dispersal and survival of larvae, the availability

of settlement habitat for spat and post-settlement survival of juveniles until successful recruitment (*Cowen and Sponaugle*, 2009). For a scallop spawned in a subpopulation, j, the probability of recruitment to a subpopulation i is dependent on all of these factors, such that the number $c_{(j,i)}$ of scallops that recruit to i per scallop spawned in subpopulation j is

$$c_{(j,i)} = p_i^r \phi_{(j,i)} p_j^l f_j \tag{B.1}$$

where f_j is the fecundity of scallops in subpopulation j, p_j^l is the relative survivorship until settlement of larvae spawned in j, $\phi_{(j,i)}$ is the fraction of larval spawned in j at are transported to i and p_i^r is the relative survivorship until recruitment of juveniles in subpopulation i.

If the number n_i of scallops in each of N subpopulations were known, then the structured population could be represented by

$$n = \begin{pmatrix} n_1 & n_2 & \cdots & n_N \end{pmatrix}^T. \tag{B.2}$$

Since the change in size of a local population is recruitment minus death, the population dynamic can be described by

$$\begin{pmatrix} n_1 \\ n_2 \\ \vdots \\ n_N \end{pmatrix} = \begin{pmatrix} c_{(1,1)} & c_{(1,2)} & \cdots & c_{(1,N)} \\ c_{(2,1)} & c_{(2,2)} & & c_{(2,N)} \\ \vdots & & \ddots & \vdots \\ c_{(N,1)} & \cdots & \cdots & c_{(N,N)} \end{pmatrix} \begin{pmatrix} n_1 \\ n_2 \\ \vdots \\ n_N \end{pmatrix} + \begin{pmatrix} p_1^a & 0 & \cdots & 0 \\ 0 & p_2^a & & 0 \\ \vdots & & \ddots & \vdots \\ 0 & 0 & \cdots & p_N^a \end{pmatrix} \begin{pmatrix} n_1 \\ n_2 \\ \vdots \\ n_k \end{pmatrix}, \tag{B.3}$$

where p_i^a is the rate of survivorship of adult scallops between spawning events. In matrix form, equation B.3 is

$$\mathbf{n} = \mathbf{Cn} + \mathbf{Pn}. \tag{B.4}$$

The matrix $\mathbf{C}$ in equation B.4 is consistent with definitions of the connectivity matrix given by *Cowen and Sponaugle* (2009). Note that in general, $\mathbf{C}$ is not truly independent of demographics and demographic processes in each subpopulation since there are many interactions between population size/structure and larval production and post-settlement success (the effects of these demographic factors are a main focus of this thesis). However, distinguishing between $\mathbf{C}$ and $\mathbf{P}$ is useful in demarcating the role that connectivity plays in the dynamics of a spatially structured population (changes in $\mathbf{n}$ over time) and in distinguishing it from demographic processes that impact subpopulations, such as density-dependent inhibition and intra-specific competition among adults. The latter effects would manifest in $\mathbf{P}$, not $\mathbf{C}$.

Post-settlement processes (p^r) were not discussed in this thesis. The connectivity matrix was not computed from simulation explicitly. In chapter 4, the effects of abundance, fecundity (combined to give f_i), adult distribution, larval behaviour, ocean currents (combined to get $\phi_{(j,i)}$) and larval mortality rate (to give p_i^l) were used along with geographic delineations of subpopulations to define a "larval connectivity matrix", $\mathbf{L}$ (section 2.4). The larval connectivity matrix is related to the connectivity matrix, but is not the same thing. The number $\mathbf{n}$ of larvae spawned in each subpopulation is also included in the entries of the matrix. It can be assumed to reflect the connectivity matrix only if post-settlement processes are assumed to be approximately equal within each subpopulation. It is possible that this assumption fails for scallops on GB some of the time, since fishery practices have varied in space (due to different management practices in Canada and the US, and due to the fishery closed areas). The larval connectivity matrix is, nonetheless, useful for describing the exchange of larvae among the subpopulations, and this concept has been defined here as "larval connectivity".

The simulations in chapter 3 neglected the fecundity, abundance (f_i) and distribution of adult scallops on GB, and mortality rates of the larvae (p_i^l). This leaves only the transport

term of equation B.1, $\phi_{(j,i)}$. Since the distribution of adults was not modelled in chapter 3, the estimates of $\phi_{(j,i)}$ made there are likely less accurate than those implicitly made in chapter 4. These quantities were termed *connection fractions*, since they represented the fraction of particles that were transported to connect one subpopulation to another. Because these terms were fractions, the resulting matrix (the "transport connectivity matrix") is a transition matrix. As for the laval connectivity matrix, the transport connectivity matrix is distinct from the connectivity matrix. However, it does describe one of the processes that contributes to population connectivity – transport – and this concept was referred to in this thesis as "transport connectivity". Transport connectivity was investigated in chapter 3 for convenience and simplicity, and offers no information about population connectivity that larval connectivity does not.

APPENDIX C

RIGHTS RELEASE FORM

The following pages contain the rights release form for the previously published content in this thesis contained in *Gilbert et al.* (2010). The results of this work are found in chapter 3, and some additional text from this work is found in chapters chapter 1 and chapter 2.

ELSEVIER LICENSE
TERMS AND CONDITIONS

Mar 07, 2011

This is a License Agreement between Chad S Gilbert ("You") and Elsevier ("Elsevier") provided by Copyright Clearance Center ("CCC"). The license consists of your order details, the terms and conditions provided by Elsevier, and the payment terms and conditions.

All payments must be made in full to CCC. For payment instructions, please see information listed at the bottom of this form.

Supplier	Elsevier Limited The Boulevard,Langford Lane Kidlington,Oxford,OX5 1GB,UK
Registered Company Number	1982084
Customer name	Chad S Gilbert
Customer address	77 Russell Lake Dr., Unit 509 Halifax, NS B2W 6R8
License number	2594291276229
License date	Jan 22, 2011
Licensed content publisher	Elsevier
Licensed content publication	Progress in Oceanography
Licensed content title	Modelling dispersal of sea scallop (*Placopecten magellanicus*) larvae on Georges Bank: The influence of depth-distribution, planktonic duration and spawning seasonality
Licensed content author	C.S. Gilbert, W.C. Gentleman, C.L. Johnson, C. DiBacco, J.M. Pringle, C. Chen
Licensed content date	October-December 2010
Licensed content volume number	87
Licensed content issue number	1-4
Number of pages	12
Start Page	37
End Page	48
Type of Use	reuse in a thesis/dissertation
Format	both print and electronic
Are you the author of this Elsevier article?	Yes
Will you be translating?	No
Order reference number	
Title of your thesis/dissertation	The Biological and Demographic Factors Driving Population Connectivity in Sea Scallop Placopecten magellanius on Georges Bank

Expected completion date	Mar 2011
Estimated size (number of pages)	100
Elsevier VAT number	GB 494 6272 12
Permissions price	0.00 USD
Value added tax 0.0%	0.0 USD / 0.0 GBP
Total	**0.00 USD**
Terms and Conditions	

INTRODUCTION

1. The publisher for this copyrighted material is Elsevier. By clicking "accept" in connection with completing this licensing transaction, you agree that the following terms and conditions apply to this transaction (along with the Billing and Payment terms and conditions established by Copyright Clearance Center, Inc. ("CCC"), at the time that you opened your Rightslink account and that are available at any time at http://myaccount.copyright.com).

GENERAL TERMS

2. Elsevier hereby grants you permission to reproduce the aforementioned material subject to the terms and conditions indicated.

3. Acknowledgement: If any part of the material to be used (for example, figures) has appeared in our publication with credit or acknowledgement to another source, permission must also be sought from that source. If such permission is not obtained then that material may not be included in your publication/copies. Suitable acknowledgement to the source must be made, either as a footnote or in a reference list at the end of your publication, as follows:
"Reprinted from Publication title, Vol /edition number, Author(s), Title of article / title of chapter, Pages No., Copyright (Year), with permission from Elsevier [OR APPLICABLE SOCIETY COPYRIGHT OWNER]." Also Lancet special credit - "Reprinted from The Lancet, Vol. number, Author(s), Title of article, Pages No., Copyright (Year), with permission from Elsevier."

4. Reproduction of this material is confined to the purpose and/or media for which permission is hereby given.

5. Altering/Modifying Material: Not Permitted. However figures and illustrations may be altered/adapted minimally to serve your work. Any other abbreviations, additions, deletions and/or any other alterations shall be made only with prior written authorization of Elsevier Ltd. (Please contact Elsevier at permissions@elsevier.com)

6. If the permission fee for the requested use of our material is waived in this instance, please be advised that your future requests for Elsevier materials may attract a fee.

7. Reservation of Rights: Publisher reserves all rights not specifically granted in the combination of (i) the license details provided by you and accepted in the course of this licensing transaction, (ii) these terms and conditions and (iii) CCC's Billing and Payment terms and conditions.

8. License Contingent Upon Payment: While you may exercise the rights licensed immediately upon issuance of the license at the end of the licensing process for the transaction, provided that you have disclosed complete and accurate details of your proposed use, no license is finally effective unless and until full payment is received from you (either by publisher or by CCC) as provided in CCC's Billing and Payment terms and conditions. If full payment is not received on a timely basis, then any license preliminarily granted shall be deemed automatically revoked and shall be void as if never granted. Further, in the event that you breach any of these terms and conditions or any of CCC's Billing and Payment terms and conditions, the license is automatically revoked and shall be void as if never granted. Use of materials as described in a revoked license, as well as any use of the materials beyond the scope of an unrevoked license, may constitute copyright infringement and publisher reserves the right to take any and all action to protect its copyright in the materials.

9. Warranties: Publisher makes no representations or warranties with respect to the licensed material.

10. Indemnity: You hereby indemnify and agree to hold harmless publisher and CCC, and their respective officers, directors, employees and agents, from and against any and all claims arising out of your use of the licensed material other than as specifically authorized pursuant to this license.

11. No Transfer of License: This license is personal to you and may not be sublicensed, assigned, or transferred by you to any other person without publisher's written permission.

12. No Amendment Except in Writing: This license may not be amended except in a writing signed by both parties (or, in

the case of publisher, by CCC on publisher's behalf).
13. Objection to Contrary Terms: Publisher hereby objects to any terms contained in any purchase order, acknowledgment, check endorsement or other writing prepared by you, which terms are inconsistent with these terms and conditions or CCC's Billing and Payment terms and conditions. These terms and conditions, together with CCC's Billing and Payment terms and conditions (which are incorporated herein), comprise the entire agreement between you and publisher (and CCC) concerning this licensing transaction. In the event of any conflict between your obligations established by these terms and conditions and those established by CCC's Billing and Payment terms and conditions, these terms and conditions shall control.
14. Revocation: Elsevier or Copyright Clearance Center may deny the permissions described in this License at their sole discretion, for any reason or no reason, with a full refund payable to you. Notice of such denial will be made using the contact information provided by you. Failure to receive such notice will not alter or invalidate the denial. In no event will Elsevier or Copyright Clearance Center be responsible or liable for any costs, expenses or damage incurred by you as a result of a denial of your permission request, other than a refund of the amount(s) paid by you to Elsevier and/or Copyright Clearance Center for denied permissions.

LIMITED LICENSE

The following terms and conditions apply only to specific license types:
15. **Translation**: This permission is granted for non-exclusive world **English** rights only unless your license was granted for translation rights. If you licensed translation rights you may only translate this content into the languages you requested. A professional translator must perform all translations and reproduce the content word for word preserving the integrity of the article. If this license is to re-use 1 or 2 figures then permission is granted for non-exclusive world rights in all languages.
16. **Website**: The following terms and conditions apply to electronic reserve and author websites:
Electronic reserve: If licensed material is to be posted to website, the web site is to be password-protected and made available only to bona fide students registered on a relevant course if:
This license was made in connection with a course,
This permission is granted for 1 year only. You may obtain a license for future website posting,
All content posted to the web site must maintain the copyright information line on the bottom of each image,
A hyper-text must be included to the Homepage of the journal from which you are licensing at http://www.sciencedirect.com/science/journal/xxxxx or the Elsevier homepage for books at http://www.elsevier.com , and
Central Storage: This license does not include permission for a scanned version of the material to be stored in a central repository such as that provided by Heron/XanEdu.
17. **Author website** for journals with the following additional clauses:
All content posted to the web site must maintain the copyright information line on the bottom of each image, and
he permission granted is limited to the personal version of your paper. You are not allowed to download and post the published electronic version of your article (whether PDF or HTML, proof or final version), nor may you scan the printed edition to create an electronic version,
A hyper-text must be included to the Homepage of the journal from which you are licensing at http://www.sciencedirect.com/science/journal/xxxxx , As part of our normal production process, you will receive an e-mail notice when your article appears on Elsevier's online service ScienceDirect (www.sciencedirect.com). That e-mail will include the article's Digital Object Identifier (DOI). This number provides the electronic link to the published article and should be included in the posting of your personal version. We ask that you wait until you receive this e-mail and have the DOI to do any posting.
Central Storage: This license does not include permission for a scanned version of the material to be stored in a central repository such as that provided by Heron/XanEdu.
18. **Author website** for books with the following additional clauses:
Authors are permitted to place a brief summary of their work online only.
A hyper-text must be included to the Elsevier homepage at http://www.elsevier.com
All content posted to the web site must maintain the copyright information line on the bottom of each image
You are not allowed to download and post the published electronic version of your chapter, nor may you scan the printed edition to create an electronic version.
Central Storage: This license does not include permission for a scanned version of the material to be stored in a central repository such as that provided by Heron/XanEdu.

19. **Website** (regular and for author): A hyper-text must be included to the Homepage of the journal from which you are licensing at http://www.sciencedirect.com/science/journal/xxxxx. or for books to the Elsevier homepage at http://www.elsevier.com
20. **Thesis/Dissertation**: If your license is for use in a thesis/dissertation your thesis may be submitted to your institution in either print or electronic form. Should your thesis be published commercially, please reapply for permission. These requirements include permission for the Library and Archives of Canada to supply single copies, on demand, of the complete thesis and include permission for UMI to supply single copies, on demand, of the complete thesis. Should your thesis be published commercially, please reapply for permission.
21. **Other Conditions**:

v1.6

Gratis licenses (referencing $0 in the Total field) are free. Please retain this printable license for your reference. No payment is required.

If you would like to pay for this license now, please remit this license along with your payment made payable to "COPYRIGHT CLEARANCE CENTER" otherwise you will be invoiced within 48 hours of the license date. Payment should be in the form of a check or money order referencing your account number and this invoice number RLNK0.
Once you receive your invoice for this order, you may pay your invoice by credit card. Please follow instructions provided at that time.

Make Payment To:
Copyright Clearance Center
Dept 001
P.O. Box 843006
Boston, MA 02284-3006

For suggestions or comments regarding this order, contact Rightslink Customer Support:
customercare@copyright.com or +1-877-622-5543 (toll free in the US) or +1-978-646-2777.

APPENDIX D

LAGRANGIAN RESIDUALS

The first description of the Lagrangian residual velocity (LRV) as a means of describing large-scale ocean circulation was offered by *Longuet-Higgins* (1969). He defined the LRV under an assumption that the phase of the tide was a linear function of space. *Zimmerman* (1979) criticized the definition by *Longuet-Higgins* (1969), arguing that the LRV should be defined as the net transport experienced by a parcel of water over one tidal period, for which the original definition was only an approximation. It is this definition that has prevailed in the literature since.

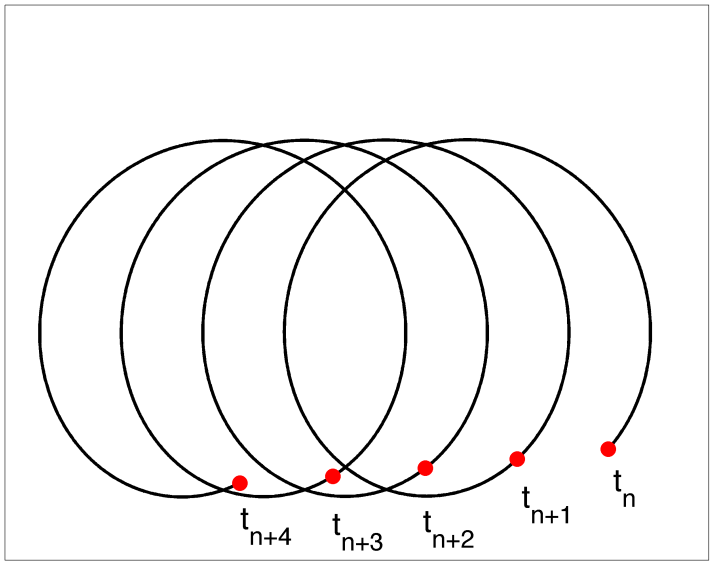

Figure D.1: The trajectory of a particle in a periodic flow with no Eulerian residual flow. The particle begins at its initial position at time t_n, and is advected by the tides. Due to spatial variation in the tidal phase or amplitude, the particle is at a new position after one full tidal period at time t_{n+1}. This is the Lagrangian residual displacement. The process continues and the particle is transported farther. This sort of displacement can occur in the absence of a mean Eulerian residual current.

D.1 Estimating the Lagrangian Residual Velocity

The appeal of using a Lagrangian residual velocity is that it allows one to describe the displacement of a water-parcel or a passive particle over a period of time. If the currents are periodic, then averaging over this period provides a time-averaged description of this transport, which will be the same on every period of the tide. This ideal situation is approximated by some regions of the ocean, wherever there is a single dominant tidal period. The circulation on GB is dominated by the M2 tide (which has a period of 12.42 hours), and thus the LRV can be used to approximate the residual circulation in this region.

Further research has gone into developing methods for estimating this quantity by applying a mathematical transform to the Eulerian residual and tidal ellipse (*Cheng and Casulli*, 1982; *Cheng et al.*, 1984; *Feng et al.*, 1986). However, an alternative computational method has also been used (*Johnson et al.*, 2006; *Banas et al.*, 2009), in which particle

trajectories are integrated in the time-varying flow field over one time-step. By performing this procedure for different phases of the tide and at numerous positions in space, the LRV can be estimated numerically. The non-linear effects which are difficult to capture in mathematical methods can be captured by these computational methods. Thus, the computational method is used in this thesis.

Particles were initialized within the model domain and high resolution, time-varying flow field simulated by FVCOM on a 1 km by 1 km square grid, with 15 particles spaced evenly in depth throughout the water-column (on σ-levels). Their trajectories were simulated according to the advection-diffusion equation over eight evenly spaced phases of the tide and averaged to give a single estimate of the LRV. The average temperature, density and kinetic mixing coefficient seen by each particle over this period were also recorded over these particle tracks. In this way, the "Lagrangian residual temperature", T, and the "Lagrangian residual water density", ρ, were defined by averaging their corresponding quantities of those tracks. The vertical mixing coefficient, k, was "averaged" by summing the product of the coefficient and the time-step, since the diffusive effect of mixing on the displacement of a particle depends on the time-scale over which the particle is dispersed.

D.2 Integrating LRV in Particle-Tracking Models

The LRV describes the quantity that is needed for modeling the transport of Lagrangian particles, and indeed transport of biota and contaminants in the ocean have often been modeled using these tidally-averaged flows (e.g. *Miller et al.*, 1998; *Lynch et al.*, 1998; *Gentleman*, 2000; *Johnson et al.*, 2006; *Banas et al.*, 2009; *Gilbert et al.*, 2010). In some of these studies, the time-step over which particle trajectories were integrated was not chosen to be the tidal period over which they were averaged. This is potentially problematic, because the LRV describes the displacement over a tidal period, and not an instantaneous

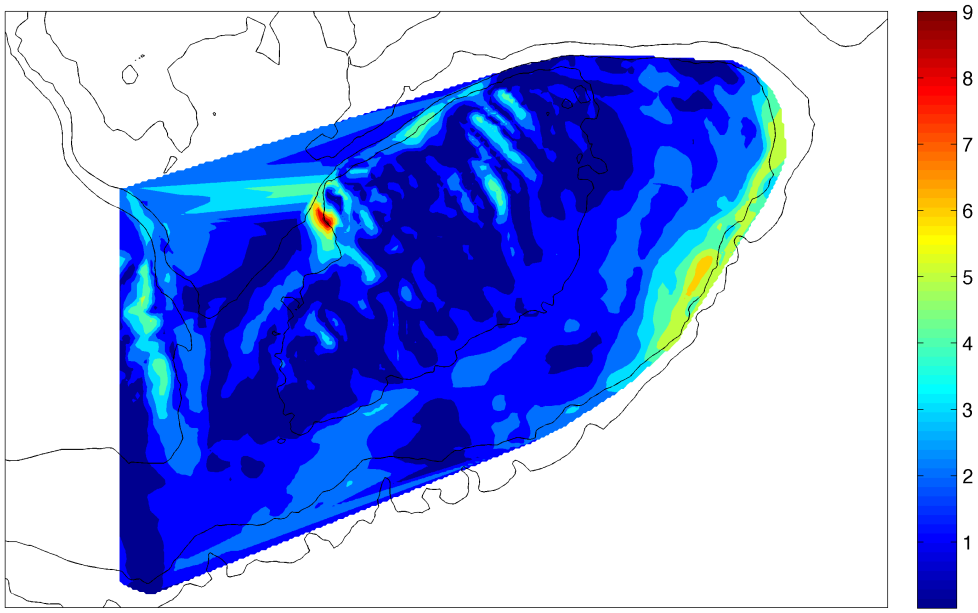

Figure D.2: The distance between particle displacement simulated with a time-step of $1/10^{th}$ of the tidal period and that for a time-step of one tidal period, on GB.

velocity. This problem may arise because this quantity is referred to as a velocity, and not a displacement. This is a useful nomenclature for describing a Lagrangian residual circulation of a region for discussion (e.g. *Pringle*, 2006; *Petersen et al.*, 2008), however, I suggest that in the context of particle-tracking, it makes more sense to consider the Lagrangian residual *displacement* instead so that it is clear that this quantity is defined over the tidal period.

To evaluate the importance of integrating the LRV in a particle-tracking simulation using the correct time-step of one period, a case study on GB was performed. The particle tracks that result from integrating with a tidal time-step were compared with particle tracks with a time-step of $1/10^{th}$ of the tidal period. Particles were seeded over all of GB within the 100 m isobath, and their drift simulated using both time-steps, assuming a *passive* swimming

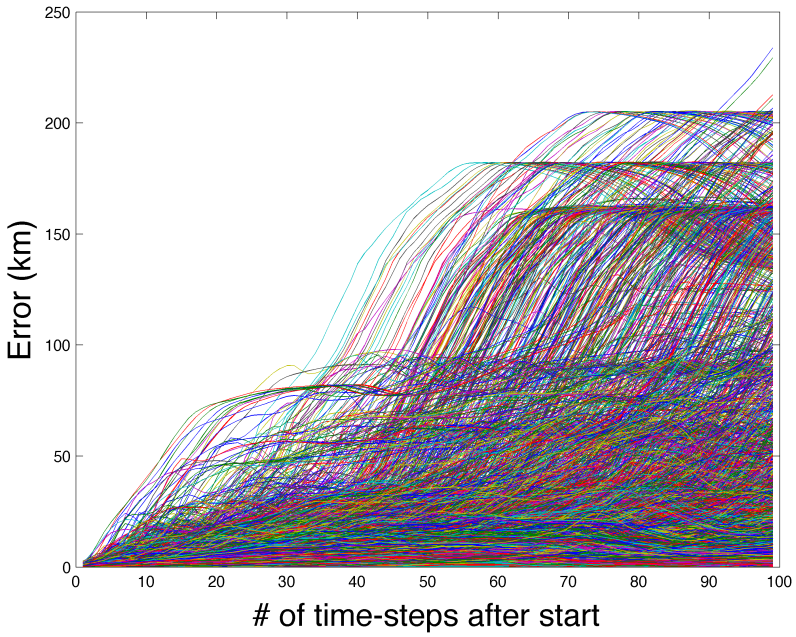

Figure D.3: The distance between particles simulated with a short time-step from their corresponding particles simulated with a tidal time-step. After 50 days, some particle pairs are hundreds of kilometers apart. The average distance between particle paris is 40 km.

behaviour in the simulated mid-September environment. The effect of the small time-step on simulated drift was evaluated by comparing the displacement of each particle after 10 time-steps (12.42 hours) with the "true" Lagrangian displacement. The magnitude of this difference was spatially-dependent and ranged between 0 to 9 km (figure D.2). The largest errors (above 5 km) occurred on the eastern edge of the NEP, on the western part of the GSC, and to the northeast of the GSC. The typical displacement of particles over one tidal period was 3.3 km, as compared to the mean error introduced by the small time-step of 1.6 km, suggesting that use of an incorrect time-step can cause significant errors in particle-tracks. To see how this error grows over time, both simulations were run for 50 days. The distance of each particle in the short time-step simulation from its corresponding particle in the tidal time-step simulation is shown in figure D.3. It is clear that simulated particle paths depend on the time-step used to compute them on GB, and that using the tidal time-step to perform this computation is crucial.

BIBLIOGRAPHY

Adams, C. F., B. P. Harris, and K. D. E. Stokesbury, Geostatistical comparison of two independent video surveys of sea scallop abundance in the Elephant Trunk Closed Area, USA, *ICES Journal of Marine Sciences*, *68*, 995–1002, 2008.

Adams, C. F., B. P. Harris, M. C. Marino II, and K. D. Stokesbury, Quantifying sea scallop bed diameter on Georges Bank with geostatistics, *Fisheries Research*, *106*, 460–467, 2010.

Ashjian, C., C. Davis, S. Gallager, and P. Alatalo, Distribution of plankton, particles, and hydrographic features across Georges Bank described using the Video Plankton Recorder, *Deep Sea Research Part II: Topical Studies in Oceanography*, *48*, 245–282, 2001.

Banas, N., P. McDonald, and D. Armstrong, Green Crab Larval Retention in Willapa Bay, Washington: An Intensive Lagrangian Modeling Approach, *Estuaries and Coasts*, *32*, 893–905, 2009.

Barber, B., R. Getchell, S. Shumway, and D. Schick, Reduced Fecundity in a Deep-Water Population of the Giant Scallop *Placopecten magellanicus* in the Gulf-of-Maine, Usa, *Marine Ecology-Progress Series*, *42*, 207–212, 1988.

Beaumont, A. R., and D. A. Barnes, Aspects of veliger larval growth and byssus drifting of the spat of Pecten maximus and Aequipecten (Chlamys) opercularis, *ICES J. Mar. Sci.*, *49*, 417–423, 1992.

Botsford, L., A. Hastings, and S. D. Gaines, Dependence of sustainability on the configuration of marine reserves and larval dispersal distance, *Ecology Letters*, pp. 144–150, 2001.

Chen, C., H. Liu, and R. Beardsley, An unstructured grid, finite-volume, three-dimensional, primitive equations ocean model: Application to coastal ocean and estuaries, *Journal of Atmospheric and Oceanic Technology*, *20*, 159–186, 2003.

Cheng, R. T., and V. Casulli, On Lagrangian residual currents with applications in south San Francisco Bay, California, *Water Resources Research*, *18*, 1652, 1982.

Cheng, R. T., V. Casulli, and S. N. Milford, Eulerian-Lagrangian Solution of the Convection-Dispersion Equation in Natural Coordinates, *Water Resources Research*, *20*, 944, 1984.

Chia, F., J. Bucklandnicks, and C. Young, Locomotion of Marine Invertebrate Larvae: A Review, 1984.

Cowen, R., and S. Sponaugle, Larval dispersal and marine population connectivity, *Annual Review of Marine Science*, *1*, 443–466, 2009.

Culliney, J., Larval development of the giant scallop *Placopecten magellanicus* (Gmelin), *Biological Bulletin*, *147*, 321–332, 1974.

Davis, C., Zooplankton life cycles, in *Georges Bank*, edited by R. Backus, pp. 256–267, MIT Press, Cambride, Mass., 1987.

DiBacco, C., G. Robert, and J. Grant, Reproductive-Cycle of the Sea Scallop, Placopecten-Magellanicus (gmelin, 1791), on Northeastern Georges-Bank, *Journal of Shellfish Research*, *14*, 59–69, 1995.

Ecker, M., and J. Heltsche, Geostatistical Estimates of Scallop Abundance., in *Case Studies in Biometry*, edited by N. Lange, L. Ryan, L. Billard, D. Brillinger, L. Conquest, and J. Greenhouse, pp. 107–124, John Wiley & Sons, New York, 1994.

Feng, S., R. T. U. G. S. Cheng, and P. S. C. O. O. Xi, On the Lagrangian residual current and residual transport 1. Lagrangian residual current, *Water Resources*, *22*, 1623–1634, 1986.

Gallager, S., J. Manuel, D. Manning, and R. ODor, Ontogenetic changes in the vertical distribution of giant scallop larvae, *Placopecten magellanicus*, in 9-m deep mesocosms as a function of light, food, and temperature stratification, *Marine Biology*, *124*, 679–692, 1996.

Gentleman, W. C., Factors controlling th seasonal abundance distribution of Calanus finmarchicus in the Gulf of Maine/Georges Bank region, Ph.d. thesis, Dartmouth College, 2000.

Gilbert, C., W. Gentleman, C. Johnson, C. DiBacco, J. Pringle, and C. Chen, Modelling dispersal of sea scallop (Placopecten magellanicus) larvae on Georges Bank: The influence of depth-distribution, planktonic duration and spawning seasonality, *Progress In Oceanography*, *87*, 37–48, 2010.

Grimm, V., K. Reise, and M. Strasser, Marine metapopulations : a useful concept ?, *Conservation Biology*, pp. 222–228, 2003.

Hart, D., Sea Scallop Stock Assessment Update for 2005. US Dep. Commer, *Northeast Fish. Sci. Cent. Ref. Doc*, pp. 06–20, 2006.

Hart, D., and A. Chute, Essential fish habitat source document: sea scallop, *Placopecten magellanicus*, life history and habitat characteristics (2nd edition), 2004.

Hart, D., and P. Rago, Long-term dynamics of US Atlantic sea scallop *Placopecten magellanicus* populations, *North American Journal of Fisheries Management*, *26*, 490–501, 2006.

Houde, E., Comparative growth, mortality and energetics of marine fish larvae, *Fishery Bulletin*, *87*, 471–495, 1989.

Houde, E., and J. Bartsch, Mortality, in *Manual of Recommended Practices for Modelling Physical-Biological Interactions During Fish Early Life.*, edited by E. North, A. Gallego, and P. Petitgas, 1 ed., chap. 4, pp. 45–62, ICES Workshop on advancements in modelling physical- biological interactions in fish early-life history, 2008.

Hunter, C., and H. Caswell, The use of the vec-permutation matrix in spatial matrix population models, *Ecological Modelling*, *188*, 15–21, 2005.

International Court of Justice, Delimitation of the Maritime Boundary in the Gulf of Maine Area (Canada/United States of America), 1984.

Johnson, C., J. Pringle, and C. Chen, Topical Studies in Oceanography : Transport and retention of dormant copepods in the Gulf of Maine, *Deep Sea Research Part II*, *53*, 2520–2536, 2006.

Kritzer, J. P., and P. F. Sale, Metapopulation ecology in the sea: from Levins' model to marine ecology and fisheries science, *Fish and Fisheries*, *5*, 131–140, 2004.

Langton, R., W. Robinson, and D. Schick, Fecundity and reproductive effort of sea scallops Placopecten magellanicus from the Gulf of Maine, *Marine Ecology Progress Series*, *37*, 19–25, 1987.

Lewis, C. V., Biological-Physical Modelling of Sea Scallop Fishery Closures, 1999.

Limeburner, R., and R. Beardsley, The seasonal hydrography and circulation over Nantucket Shoals, *Journal of Marine Research*, pp. 371–406, 1982.

Longuet-Higgins, M., On the Transport of Mass by Time-Varying Currents, *Deep Sea Research*, *16*, 431–447, 1969.

Lough, R., and J. Manning, Tidal-front entrainment and retention of fish larvae on the southern flank of Georges Bank, *Deep-Sea Research II*, *48*, 631, 2001.

Lynch, D., W. Gentleman, D. McGillicuddy Jr, and C. Davis, Biological/physical simulations of Calanus finmarchicus population dynamics in the Gulf of Maine, *MEPS*, *169*, 189–210, 1998.

Manuel, J., and R. O'Dor, Vertical migration for horizontal transport while avoiding predators: I. A tidal/diel model, *Journal of plankton research*, *19*, 1929, 1997.

Manuel, J., S. Gallager, C. Pearce, D. Manning, and R. O'Dor, Veligers from different populations of sea scallop *Placopecten magellanicus* have different vertical migration patterns, *Marine Ecology Progress Series*, *142*, 147–163, 1996.

Mcgarvey, R., F. M. Serchuk, and I. A. McLauren, Spatial and Parent-Age Analysis of Stock-Recruitment in the Georges Bank Sea Scallop (*Placopecten magellanicus*) Population, *Canadian Journal of Fisheries Aquatic Sciences*, *50*, 564–574, 1993.

Metaxas, A., and M. Saunders, Quantifying the" Bio-" components in biophysical models of larval transport in marine benthic invertebrates: advances and pitfalls, *The Biological Bulletin*, *216*, 257, 2009.

Miller, C., D. Lynch, F. Carlotti, W. Gentleman, and C. Lewis, Coupling of an individual-based population dynamic model of Calanus finmarchicus to a circulation model for the Georges Bank region, *Fisheries Oceanography*, *7*, 219–234, 1998.

Naidu, K. S., and G. Robert, Fisheries Sea Scallop, *Placopecten magellanicus*, in *Scallops: Biology, Ecology and Aquaculture*, edited by S. Shumway and G. Parsons, 1987, 2 ed., chap. 15, pp. 869–905, Elsevier, 2006.

Naimie, C., R. Limeburner, C. Hannah, and R. Beardsley, On the geographic and seasonal patterns of the near-surface circulation on Georges Bank âĂŤ from real and simulated drifters1, *Deep Sea Research Part II: Topical Studies in Oceanography*, *48*, 501–518, 2001.

Naimie, C. E., J. W. Loder, and D. R. Lynch, Seasonal Variation of the three-dimensional circulation on Georges Bank, *Journal of Geophysical Research*, *99*, 15,967–15,989, 1994.

Neuheimer, A., and C. Taggart, The growing degree-day and fish size-at-age: the overlooked metric, *Canadian Journal of Fisheries and Aquatic Sciences*, *64*, 375–385, 2007.

O'Reilly, J. E., and C. Zetlin, Seasonal, horizontal, and vertical distribution of phytoplankton chlorophyll a in the northeast US continental shelf ecosystem, 1998.

Orensanz, J., A. Parma, T. Turk, and J. Valero, Dynamics, assessment and man- agement of exploited natural populations., in *Scallops: Biology, Ecology and Aquaculture*, edited by S. Shumway and G. J. Parsons, 2 ed., pp. 756–868, Elsevier, Amsterdam, 2006.

Petersen, L., H. Muller, and V. Mariette, Estimating Lagrangian Residual Circulation (LRC) in the Iroise Sea, in *Current Measurement Technology, 2008. CMTC 2008. IEEE/OES 9th Working Conference on*, pp. 279–284, IEEE, 2008.

Pineda, J., J. Hare, and S. Sponaungle, Larval transport and dispersal in the coastal ocean and consequences for population connectivity, *Oceanography*, *20*, 22–39, 2007.

Posgay, J., Movement of tagged sea scallops on Georges Bank, *Marine Fisheries Review*, *43*, 19–25, 1981.

Posgay, J., and K. Norman, An Observation on the Spawning of the Sea Scallop, Placopecten magelhznicus (Gmelin), on Georges Bank, *Limnology and Oceanography*, *3*, 478–478, 1958.

Pringle, J., Sources of variability in Gulf of Maine circulation, and the observations needed to model it, *Deep Sea Research Part II: Topical Studies in Oceanography*, *53*, 2457–2476, 2006.

Ribeiro Jr, P., and P. Diggle, geoR: A package for geostatistical analysis, *R News*, *1*, 15–18, 2001.

Savina, M., G. Lacroix, and K. Ruddick, Modelling the transport of common sole larvae in the southern North Sea: Influence of hydrodynamics and larval vertical movements, *Journal of Marine Systems*, *81*, 86–98, 2010.

Scheffer, M., Super-individuals a simple solution for modelling large populations on an individual basis, *Ecological Modelling*, *80*, 161–170, 1995.

Stewart, P., and S. Arnold, Environmental requirements of the sea scallop (*Placopecten magellanicus*) in eastern Canada and its response to human impacts., *Canadian Technical Report of Fisheries and Aquatic Sciences*, p. 36, 1994.

Stokesbury, K., B. Harris, M. Marino, and J. Nogueira, Estimation of sea scallop abundance using a video survey in off-shore US waters, *Journal of Shellfish research*, *23*, 33–40, 2004.

Thomson, R., and I. Fine, Estimating mixed layer depth from oceanic profile data, *Journal of Atmospheric and Oceanic Technology*, *20*, 319–329, 2003.

Thouzeau, G., G. Robert, and S. Smith, Spatial variability in distribution and growth of juvenile and adult sea scallops *Placopecten magellanicus*(Gmelin) on eastern Georges Bank(Northwest Atlantic)., *Marine ecology progress series. Oldendorf*, *74*, 205–218, 1991.

Tian, R., C. Chen, K. Stokesbury, B. Rothschild, Q. Xu, S. Hu, G. Cowles, B. Harris, and M. Marino, Sensitivity analysis of sea scallop (*Placopecten magellanicus*) larvae trajectories to hydrodynamic model configuration on Georges Bank and adjacent coastal regions, *Fisheries Oceanography*, *18*, 173–184, 2009c.

Tian, R. C., C. Chen, K. D. E. Stokesbury, B. J. Rothschild, G. W. Cowles, Q. Xu, S. Hu, B. P. Harris, and M. C. Marino II, Modeling the connectivity between sea scallop population in the Middle Atlantic Bight and over Georges Bank, *Journal of Atmospheric and Oceanic Technology*, *380*, 147–160, 2009a.

Tian, R. C., C. Chen, K. D. E. Stokesbury, B. J. Rothschild, G. W. Cowles, Q. Xu, S. Hu, B. P. Harris, and M. C. Marino, Dispersal and settlement of sea scallop larvae spawned in the fishery closed areas on Georges Bank, *ICES Journal of Marine Science*, *66*, 2155–2164, 2009b.

Tremblay, M., and M. Sinclair, Sea Scallop Larvae *Placopecten magellanicus* on Georges Bank - Vertical Distribution in Relation to Water Column Stratification and Food, *Marine Ecology-Progress Series*, *61*, 1–15, 1990.

Tremblay, M. J., and M. Sinclair, Planktonic sea scallop larvae (*Placopecten magellanicus*) in the Georges Bank region: Broadscale distribution in relation to physical oceanography, *Canadian Journal of Fisheries Aquatic Sciences*, *49*, 1597–1615, 1992.

Tremblay, M. J., J. Loder, F. Werner, and CE, Drift of sea scallop larvae *Placopecten magellanicus* on Georges Bank: A model study of the roles of mean advection, larval behavior and larval origin, *Sea Research Part II: Topical Studies in Oceanography*, *41*, 7–49, 1994.

Visser, A., Using random walk models to simulate the vertical distribution of particles in a turbulent water column, *Marine Ecology Progress Series*, *158*, 275–281, 1997.

Werner, F., F. Page, D. Lynch, J. Loder, R. Lough, R. Perry, D. Greenberg, and M. Sinclair, Influences of mean advection and simple behavior on the distribution of cod and haddock early life stages on Georges Bank, *Fisheries Oceanography*, *2*, 43–64, 1993.

Werner, F. E., R. K. Cowen, and C. B. Paris, Present capabilities and necessary developments for future studies of populaiton connectivity, *Oceanography*, *20*, 54–69, 2007.

Zimmerman, J., On the Euler-Lagrange transformation and the stokes' drift in the presence of oscillatory and residual currents, *Deep Sea Research Part A. Oceanographic Research Papers*, *26*, 505–520, 1979.